THE UNIVERSITY OF MICHIGAN

COLLEGE OF ENGINEERING
Department of Electrical Engineering
Space Physics Research Laboratory

ORA Project 06093

PITOT MEASUREMENTS ON AN X-15 ROCKET PLANE

by

Jack J. Horvath
Gary F. Rupert

Contract No. AF 19(628)-3313
Project No. 6020
Task No. 602002
Work Unit No. 60200201

FINAL REPORT

Period Covered: 1 October 1963 through 31 March 1968

August 1968

Contract Monitor: Gerard A. Faucher
Aerospace Instrumentation Laboratory

Prepared
for

AIR FORCE CAMBRIDGE RESEARCH LABORATORIES
OFFICE OF AEROSPACE RESEARCH
UNITED STATES AIR FORCE
BEDFORD, MASSACHUSETTS 01730

administered through:

OFFICE OF RESEARCH ADMINISTRATION ANN ARBOR, MICHIGAN 48105

ACKNOWLEDGMENTS

The authors with to express their appreciation to R. W. Simmons (Space Physics Research Laboratory) for this contribution relating to the environmental temperatures encountered by the instrumentation during an X-15 flight and to P. A. Handy (Space Physics Research Laboratory) for his work associated with the implementation of a radioactive ionization gage for atmospheric density measurements. Also the authors thank the personnel at the NASA Flight Research Center, Edwards Air Force Base, California, for their excellent cooperation during the entire research effort.

ABSTRACT

A research project was planned as a feasibility study to determine whether the X-15 rocket plane could be adapted to carry an instrumented package for pitot measurements. To achieve the desired measurements, a wing pod modification provided the necessary internal volume and external aerodynamic geometry to permit pitot measurements of atmospheric density throughout the altitude range up to 85 km. Five flights, the first two being test flights, were made. Only the third and last flights may be considered useful in deriving results indicative of possible future application of the X-15 for purposes of obtaining reliable data for the pitot measurement. The significant aspects of the research project are the instrumentation associated with the installation of radioactive ionization gages in the X-15, the design of the nose tip configuration compatible with the X-15 wing pod design, and the replacement of the original ionization gages with more advanced models. The basic objective of obtaining accurate atmospheric density profiles to expand our understanding of the structure of the upper atmosphere was never fully attained. The present report presents the limitations preventing a successful conclusion of the research as originally conceived. However, the research effort was valuable in pointing out some of the restrictions associated with a manned rocket vehicle.

TABLE OF CONTENTS

	Page
LIST OF FIGURES	vi
1. INTRODUCTION	1
2. PROCEDURE	3
3. INSTRUMENTATION	9
3.1. Pitot Sensing System	9
3.2. Converter Deck Module	9
3.3. Heater Control Module	10
3.4. Power Supply	10
3.5. Thermistor and Calibration Supply	11
3.6. Calibration Timer	11
3.7. Temperature Control Circuit	12
4. MEASUREMENT TECHNIQUE	23
4.1. Undisturbed Free Stream Probe Environment	23
4.2. Errors due to Contamination	23
4.2.1. B-52 environment	24
4.2.2. X-15 environment	24
4.3. Other Possible Sources of Error	25
4.3.1. Trajectory	25
4.3.2. Angle of attack	26
4.3.3. Atmospheric winds	27
4.3.4. Gage and amplifier response	28
4.3.5. Calibration of the gage	28
5. DISCUSSION	38
6. BIBLIOGRAPHY	40

LIST OF FIGURES

Figure		Page
1.	The X-15 wing pod.	2
2.	Deviation of density from U.S. Standard Atmosphere, 1962, 26 February 1965.	5
3.	Deviation of density from U.S. Standard Atmosphere, 1962, 1 November 1966.	6
4.	Deviation of pressure from U.S. Standard Atmosphere, 1962, 1 November 1966.	7
5.	Ambient temperature versus altitude, 1 November 1966.	8
6.	System block diagram.	14
7.	Converter deck module.	15
8.	Heater control module.	16
9.	DC-DC converter power supply.	17
10.	Thermistor and calibration supply circuit.	18
11.	Calibration timer output format and relay switch timing.	19
12.	Calibration timer.	20
13.	Heater control switching circuit.	21
14.	Gage and amplifier environmental temperature-time history, 26 February 1965.	22
15.	Typical bow shock angle above 30 km.	30
16.	The X-15 wing pod and B-52 engine nacelle.	31
17.	Location of reaction control system components in X-15.	32
18.	Reaction motor influence on the bow shock angle.	33

LIST OF FIGURES (Concluded)

Page

Figure

19. Typical X-15 launch time trajectory parameters. 34

20. The X-15 operating area. 35

21. Impact pressure sensor and amplifier location. 36

22. Gage output response. 37

1. INTRODUCTION

From the latter part of 1963 until the spring of 1968 the Space Physics Research Laboratory, Department of Electrical Engineering, The University of Michigan, in cooperation with the Electronic Systems Division, Air Force Systems Command, has been engaged in experimental research involving pitot measurements on an X-15 rocket plane. The X-15 aircraft evolved from a succession of experimental manned aircraft, the first of which was the X-1. As the X-15 program progressed, it became apparent that the aircraft, because of its high altitude capability, could also be employed as a means of carrying compatible scientific instruments into the upper atmosphere for the purpose of measuring atmospheric structure. To meet the requirements of most atmospheric sounding instrumentations, a wing pod was installed on each wing of the X-15 (Figure 1). The basic plan was to place the wing pods in a region generally unobstructed by the flow field of the X-15 itself, thereby permitting measurement of a previously undisturbed atmosphere. Three of these rocket-powered aircraft have been used for the purpose of investigating environmental conditions associated with supersonic flight.

Ambient atmospheric densities can be resolved from pitot measurements (impact pressure) taken on a supersonic probe (Ainsworth, et al., 1961; Horvath, et al., 1962). The X-15 rocket-powered aircraft has the capability of attaining peak velocities in excess of 5000 ft/sec and altitudes exceeding 270,000 ft or approximately 82 km. Thus, from trajectory considerations alone, the X-15 aircraft seems ideally suited both for stratospheric and mesospheric measurement of ambient atmospheric density. Larson and Montoya (1964) have reported measured densities obtained by the use of research instrumentation installed as part of the basic X-15 research program. Their impact pressure measurements have been obtained from the stagnation port of the X-15 airflow sensor. The ball nose airflow sensor in the bow of the aircraft is a pressure-nulling servomechanism used for sensing the attitude of the vehicle. Because of instrumental considerations, Larson and Montoya's measured densities were limited to altitudes below 65 km.

The bow of the X-15 is certainly the most desirable region for a pitot measurement. That region, however, is not accessible to instrumentations other than those used in the normal X-15 program. The wing pod modification noted above provided the necessary internal volume and external aerodynamic geometry to permit, at least theoretically, measurements of atmospheric density throughout the entire altitude range of the X-15. The intended goal of obtaining atmospheric density profiles on a regular basis to increase our understanding of the structure of the upper atmosphere was never fully attained. Analysis of the limitations preventing a successful conclusion of the original intended effort make up the main body of the present report. The research activity undertaken here was valuable if for no other reasons than to point out the numerous restrictions associated with a manned rocket vehicle.

Figure 1. The X-15 wing pod.

2. PROCEDURE

Location of the impact pressure sensor and amplifier electronics (Section 3.1) is shown in Figure 21. A description of the associated electronic modules and radioactive gage characteristics is found in Sections 3 and 4.

X-15 flights instrumented with air density gages took place a total of five times according to the following schedule.

8 October 1964	Environment test—no source
15 December 1964	Environment test—no source
26 February 1965	First active flight
6 May 1966	Malfunction of aircraft
1 November 1966	First normal flight

The first two test flights were undertaken as a means of assuring safe environmental temperature conditions throughout the entire X-15 flight history. These flights were necessary precautions taken because of the radioactive material used in the ionization gage. Thermistors located in the ionization gage chamber were used to monitor the temperature. A temperature—time history for a typical X-15 flight is shown in Figure 14 in Section 3.7. With the exception of the radioactive source, all of the related electronic components necessary for the density measurement were included in these first flights.

The third flight was the first flight undertaken with the radioactive source. Impact pressure data were recovered in the altitude range 22-42 km. The flight objectives were for a high-speed, low-altitude trajectory and engine burnout. The X-15 28 V power source, deviating markedly from its quiescent value, caused severe perturbations in the amplifier output data above 34 km. The impact pressure below 30 km was greater than 200 torr and, for that particular ionization gage, was highly nonlinear. As a result, the pitot measurement, while indicating possible future application on the X-15 aircraft, was suspect. Figure 2 shows the density deviation for the third flight relative to the U.S. Standard Atmosphere, 1962.

The fourth instrumented X-15 flight took place on 6 May 1966. An engine malfunction necessitated emergency procedures to be carried out whereby the X-15 landed on its predetermined emergency dry lake landing field. During the landing procedure, the ionization gage was damaged when sand was ingested into the ionization gage chamber. No scientific or engineering data were derived from this test.

The fifth X-15 flight, instrumented with a radioactive ionization gage, occurred on 1 November 1966. Most of the information included in Section 4

of this report was derived from the results of the fifth flight. Figures 3, 4, and 5 show the ambient density, ambient pressure, and ambient temperature derived from the pitot measurement. The ambient pressure and temperature profiles were obtained by integrating the density profile (Simmons, 1964).

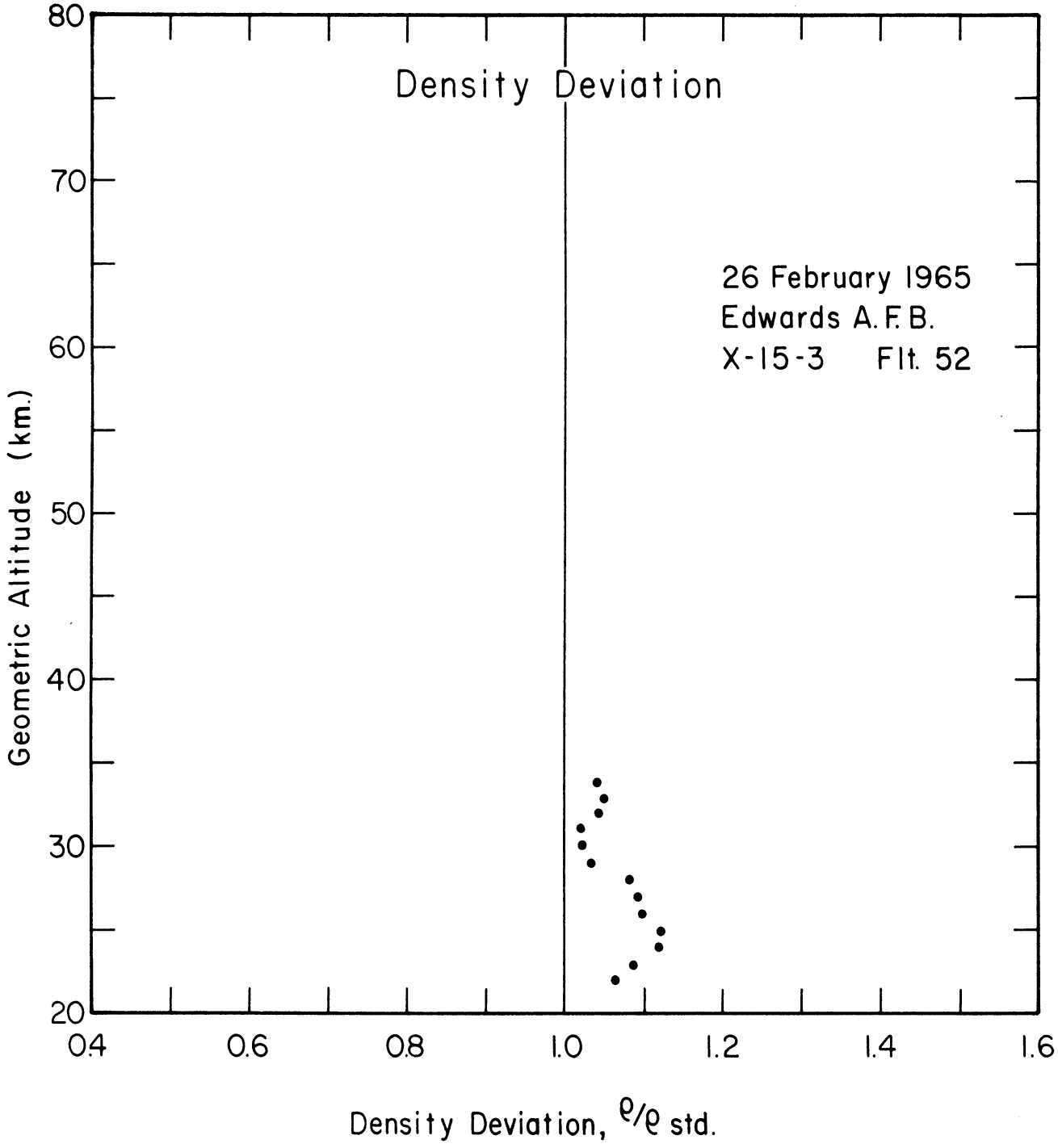

Figure 2. Deviation of density from U.S. Standard Atmosphere, 1962, 26 February 1965.

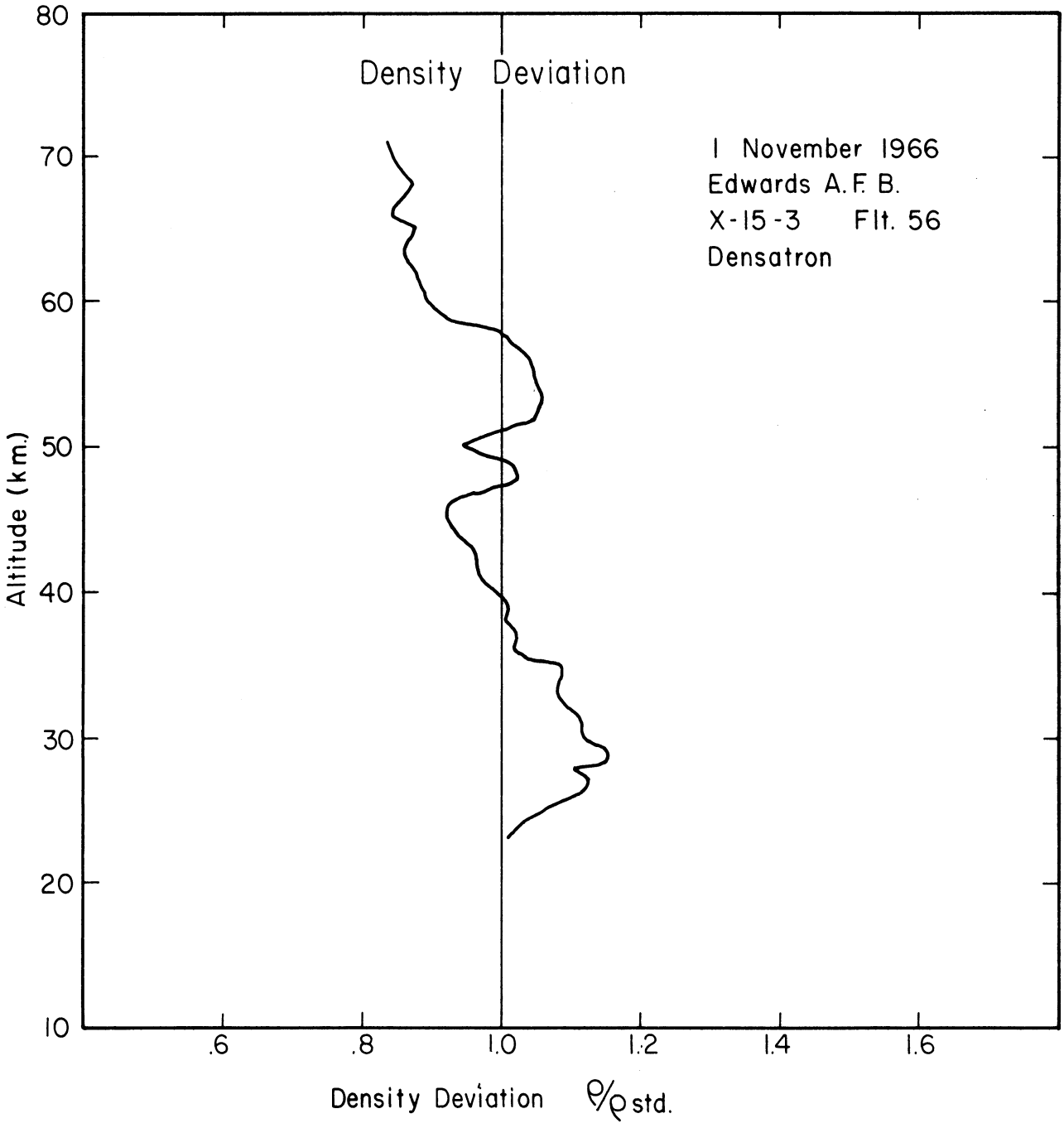

Figure 3. Deviation of density from U.S. Standard Atmosphere, 1962, 1 November 1966.

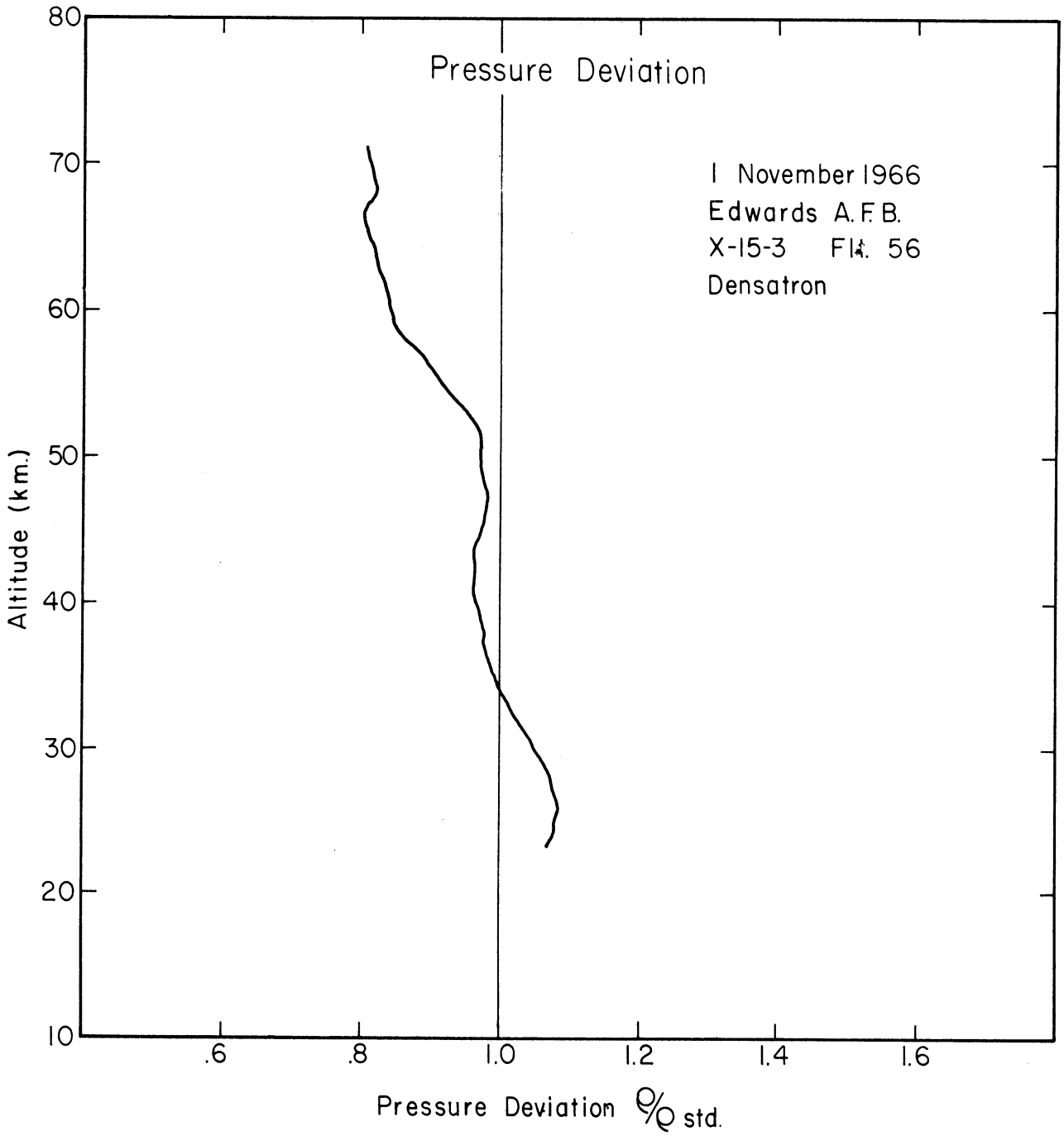

Figure 4. Deviation of pressure from U.S. Standard Atmosphere, 1962, 1 November 1966.

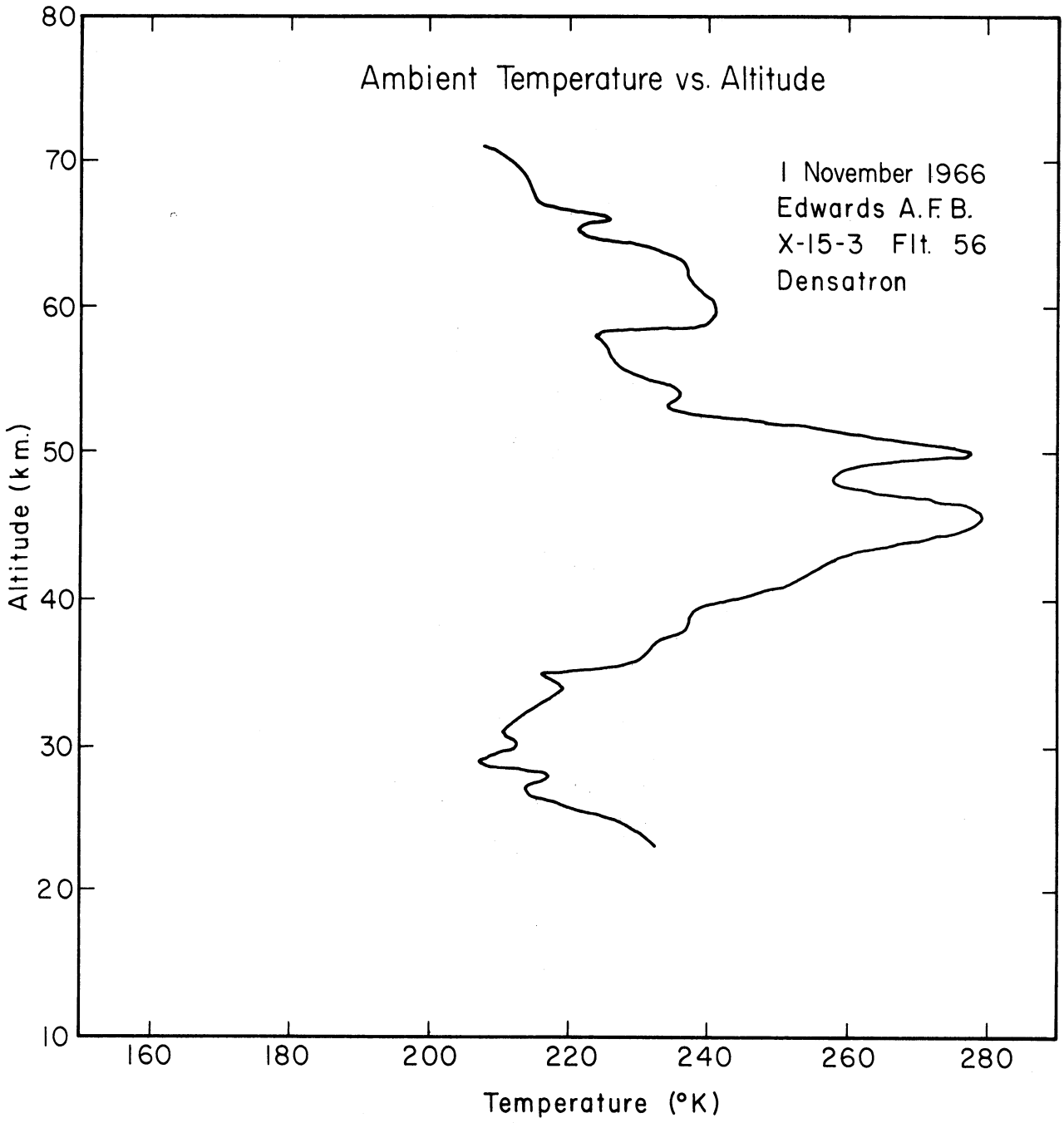

Figure 5. Ambient temperature versus altitude, 1 November 1966.

3. INSTRUMENTATION

The instrumentation required to perform the measurements is composed of a radioactive ionization gage (El-Moslimany, 1960), a multirange electrometer amplifier, a DC-DC converter module, and a heater control module. The radioactive ionization gage and the electrometer amplifier are an integral unit used to sense the impact pressure; the DC-DC converter module contains a power supply and other circuits needed to integrate the sensing system with the X-15; and the heater control module provides a means of controlling the temperature environment of the wing-mounted electronic modules. A description of each module follows. The system block diagram is shown in Figure 6.

3.1. PITOT SENSING SYSTEM

Basically, the system is composed of a multirange DC amplifier that measures low currents (as low as 10^{-12} A) from a radioactive ionization pressure gage and converts the information to a voltage (0 to +5 V DC) suitable for recording or telemetering. Besides the pressure data, the gage temperature and the amplifier range indication must also be recovered for proper reduction of the data. It is also desirable to measure the temperature of the amplifier section because of the possible extreme temperature environment.

The major design effort for the sensing system involved fitting the amplifier and gage assembly to the nose tip and the impact pressure chamber and thermally isolating them from aerodynamic heating. Another consideration was to provide a proper temperature environment for the sensing electronics before launch from the B-52, when the X-15 was subjected to outside air temperatures of about -50°C at 45,000 ft.

To solve both problems, the electrometer amplifier and the gage were first wrapped in alternate layers of Armalon and aluminum foil (usually three each) which limited radiation effects. Then fiberglass insulation was used to reduce heat conduction to or from the package. A 50 W heater-tape, placed around the gage assembly, and a 7 W heater-tape under the fiberglass around the amplifier section were used to maintain a more favorable temperature environment.

3.2. CONVERTER DECK MODULE

Located in the instrument bay just behind the pilot compartment, the converter deck module provides most of the integration functions between the wing pod and the instrument bay. All lead wiring from the electrometer amplifier goes directly to the converter module before distribution to other points (Figure 7).

Two main functions of the converter deck are to convert the raw X-15 power to a ±1 percent regulated +28 V power source and to provide in-flight voltage calibration for pressure data. A DC-DC converter circuit, explained in Section 3.4, provides the power conversion, while a calibration timer and a voltage regulator circuit, explained in Section 3.6, provide the calibration for the data.

During installation the amplifier and the converter deck may be operated independently from the X-15 system by substituting a control console in place of the X-15 input cable. After installation, the entire system may be monitored in a flight condition through a test plug provided on the top of the converter deck.

3.3 HEATER CONTROL MODULE

Control circuits and relays for the amplifier and the gage heater-tapes are mounted in the heater control module (Figure 8). The doughnut-shaped deck is then fastened to a mounting platform in the wing pod section just to the rear of the amplifier. The electrometer amplifier actually protrudes a short way into the center hole of the module. Two Cannon DEM series connectors are provided on the top side of the module for input and output lead connectors.

3.4. POWER SUPPLY

The power supply is designed to provide a relatively constant output voltage over a large change in input voltage. Since the amplifier is designed to operate above 26 V, a DC-DC converter is needed to increase the available working voltage from the X-15, which can conceivably drop as low as 24 V.

The circuit shown in Figure 9 is a standard square core oscillator operating at about 7 kHz, which has both primary and secondary regulation. The primary regulator, composed of D1, D2, and D3, keeps the ON transistor of the converter (Q1 or Q2) out of the saturation region by clamping the collector voltage. The peak-to-peak square wave voltage to the transformer primary is then held constant to a voltage equal to twice the voltage drop across D1 and D3 (or D2 and D3). The ON transistor collector/emitter voltage is equal to the difference between the input supply voltage and the drop across D1 and D3 (or D2 and D3). Added heat dissipation in Q1 and Q2, which is the cost of regulation, then results. Diodes D4 and D5 protect the base/emitter juctions of Q1 and Q2 from damaging reverse bias voltages.

Although the primary regulator has excellent input regulation, it unfortunately has poor load regulation. Therefore, a secondary regulator is needed to provide the 28 V output. A standard series regulator using two transistors in a Darlington connection (Q3 and Q4) provides sufficient load

regulation. Since the secondary supply voltage is nearly constant because of primary regulation, the collector of Q4 may be biased near the desired output voltage. In this case a collector voltage of 30 V is used. Total regulation of the circuit is about ±1 percent with an input change from 22 to 30 V, a load change from 0 to 200 mA, and a temperature change from 10 to 50° C.

3.5. THERMISTOR AND CALIBRATION SUPPLY

Reference voltages for temperature-measuring circuits and the 5 V data calibration are derived from resistive voltage-divider networks and the regulator circuit shown in Figure 10. The design utilizes an RA1B (General Electric) reference amplifier in a series regulator that supplies an 8 V source regulated to ±0.1 percent. Under normal operation, the input is already regulated to ±0.1 percent and the load current is not expected to change more than 2 mA. Therefore, the main requirement of the regulator is for regulation of the temperature.

Regulation of the temperature is accomplished by biasing the RA1B reference amplifier to obtain a low temperature drift. Each RA1B can be expected to have a different coefficient region for zero temperature, so that oven-testing is required to find the best operating points. This particular circuit will keep the output stable to ±0.1 percent by using a Zener current of 5 mA and a collector current of 1 mA.

3.6. CALIBRATION TIMER

The timing format for the calibration timer is shown in Figure 11. The circuit shown in Figure 12 uses two relays to perform the calibration function. The total calibration time is controlled by RY-1, while RY-2 changes the calibration voltage from 0 V to 5 V. A Shockley diode relaxation regulator energizes RY-1 once every 100 sec for about 200 msec. A set of contacts on RY-1 is used to energize RY-2 through a 100 msec delay circuit composed of R3 and C2.

The calibration OFF time is determined by the charging of C1 through R1 until the breakdown voltage of the Shockley oscillator is reached which is

$$t_{OFF} = R1C1 \ln \frac{E_s}{E_s - E_B} \qquad (3.1)$$

where E_s equals the supply voltage (28 V) and E_B is the breakdown voltage of the Shockley oscillator. For the values given, the OFF time is 100.3 sec.

The calibration ON time is controlled by the discharge of C1 by the parallel combination of R2 and the resistance of RY-1. If the Shockley oscillator resistance and the relay inductance are ignored, then the relation is

$$t_{ON} = R_p C1(\ell n\ E_B/E_D) \qquad (3.2)$$

where R_p is the parallel resistance of R_2 and RY-2, E_B is again the breakdown resistance of the Shockley oscillator, and E_D equals the relay dropout voltage, which is about 3.5 V. It is assumed that the minimum discharge current is above the Shockley oscillator holding current. For the value given and a relay resistance of 600 Ω, the ON time is 0.23 sec.

The delay time for RY-2 is determined by the relation

$$t_{delay} = R_T\ C_2\ \ell n \frac{E_T}{E_T - E_p} \qquad (3.3)$$

where

$$R_T = \frac{R_{relay} R_3}{R_{relay} + R_3}, \quad E_T = \frac{R_{relay}}{R_{relay} + R_3}\ E_s,$$

and E_p is the pull-in voltage of the relay which is about 11 V. By using the values shown in Figure 11, the delay time is 106 msec.

Data of a typical performance for the circuit are listed below. For best results, the supply voltage must be kept stable near 28 V. No attempt has been made to compensate the OFF time for temperature, which is largely dependent on the value of C1 (given a stable supply voltage).

	0 V Calibration Time, msec	5 V Calibration Time, msec	OFF Time, sec
10°C	(78)<u>125</u>(113)	(93)<u>125</u>(140)	88.2
27°C	(93)<u>117</u>(140)	(109)<u>125</u>(148)	96.6
50°C	(101)<u>117</u>(148)	(78)<u>117</u>(140)	100.8

Note: The underlined values are for a 28 V supply. Values for a 26 V supply and a 30 V supply are listed respectively in parentheses before and after the 28 V values.

3.7. TEMPERATURE CONTROL CIRCUIT

The power supplied to each heater-tape is controlled through a relay by a closed-loop circuit for temperature control. A temperature sensor located near each heater-tape forms one arm of a Wheatstone bridge which in turn is connected to a differential amplifier switch that controls the heater relay. The circuit is shown in Figure 13. R1, R2, R5, and R6 form the bridge where

R2 is a thermistor circuit with a positive temperature coefficient. The base voltage of Q2, determined by R5 and R6, also sets the amplifier switch point at about 7 V. The relay is normally off until the voltage on the base of Q1, caused by a decrease in the resistance of R2, becomes less than the base voltage of Q2. At this time Q2 starts to conduct and in turn causes Q1 to conduct. Thus, Q3 and the relay are turned on.

The pull-in and dropout currents of the relay, which are 18 mA and 6 mA, respectively, primarily determine the turn-on and turn-off resistance of the thermistor. The difference between the two values, roughly 200 Ω, corresponds to a temperature difference of 1°C.

Typical bias voltages for the circuit are listed below.

V Supply	Condition	Nominal Temperature	R2	VB1	VB3	VC3=V Relay
28	OFF	26.5°C	25 kΩ	6.84	27.8	0.14
28	Switch	25 °C	21.4kΩ	6.38	22.23	10.4
28	ON	24.2°C	20 kΩ	6.22	20.5	15.3

A temperature-time history for a typical X-15 flight is shown in Figure 14.

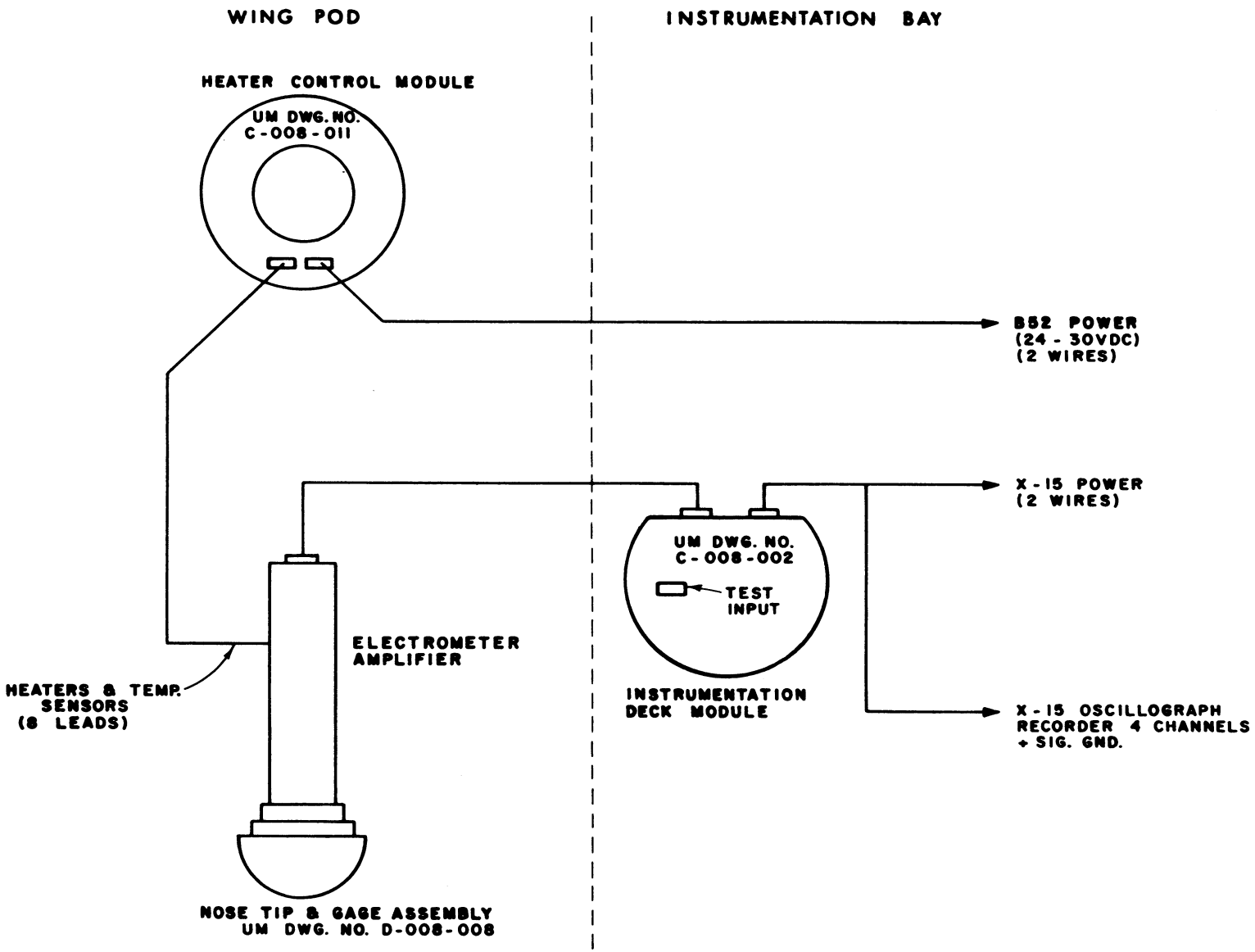

Figure 6. System block diagram.

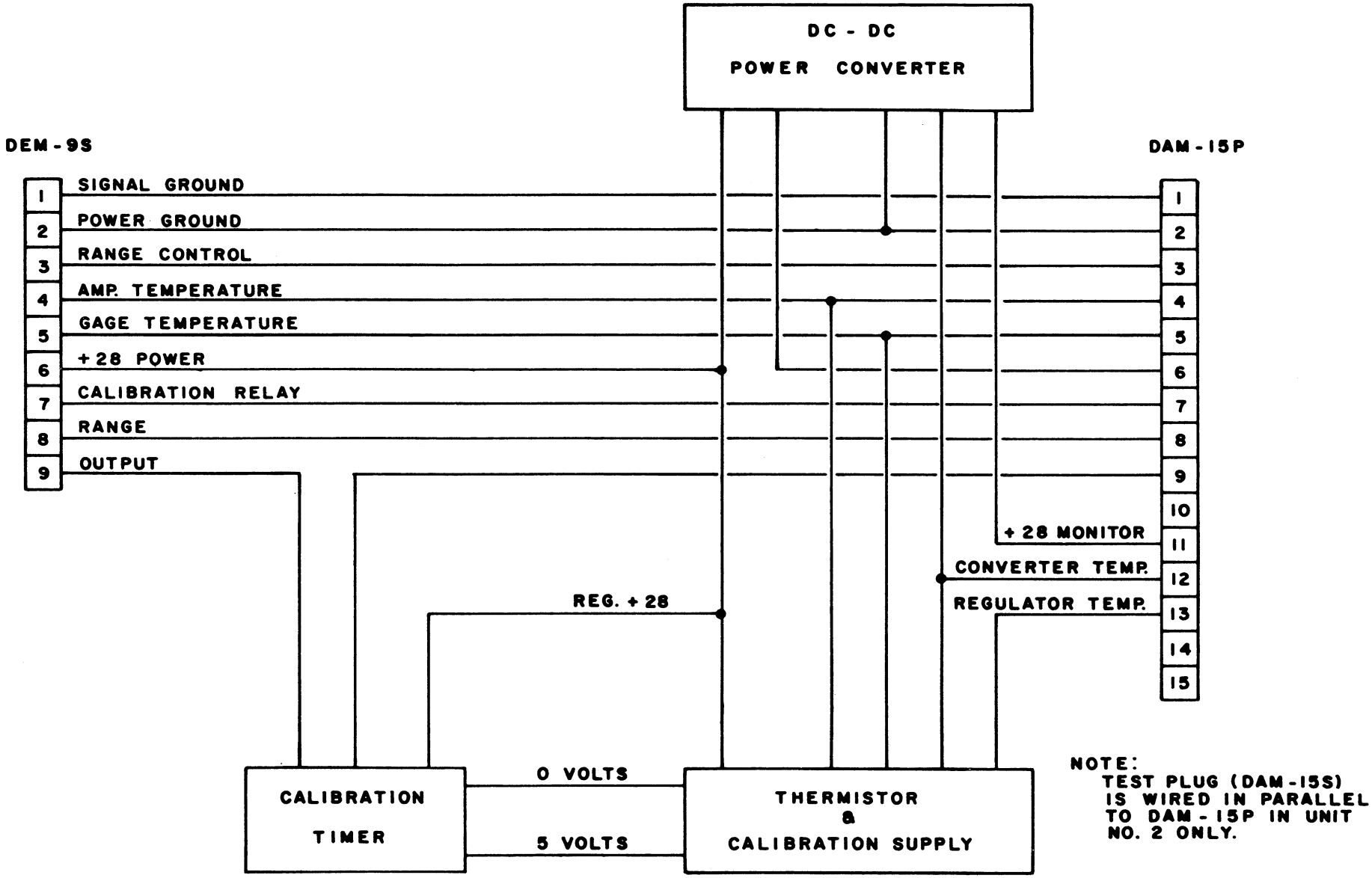

Figure 7. Converter deck module.

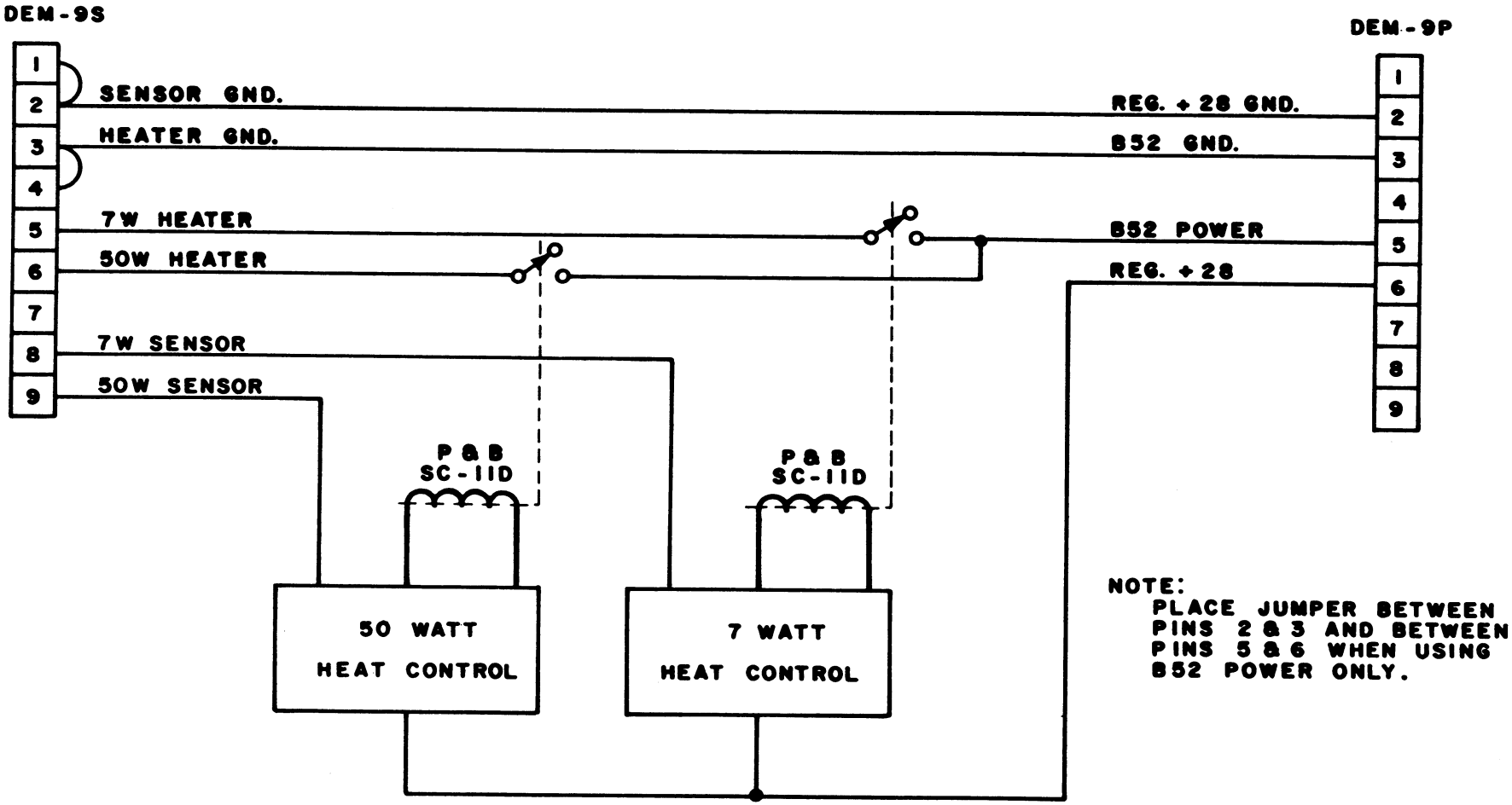

Figure 8. Heater control module.

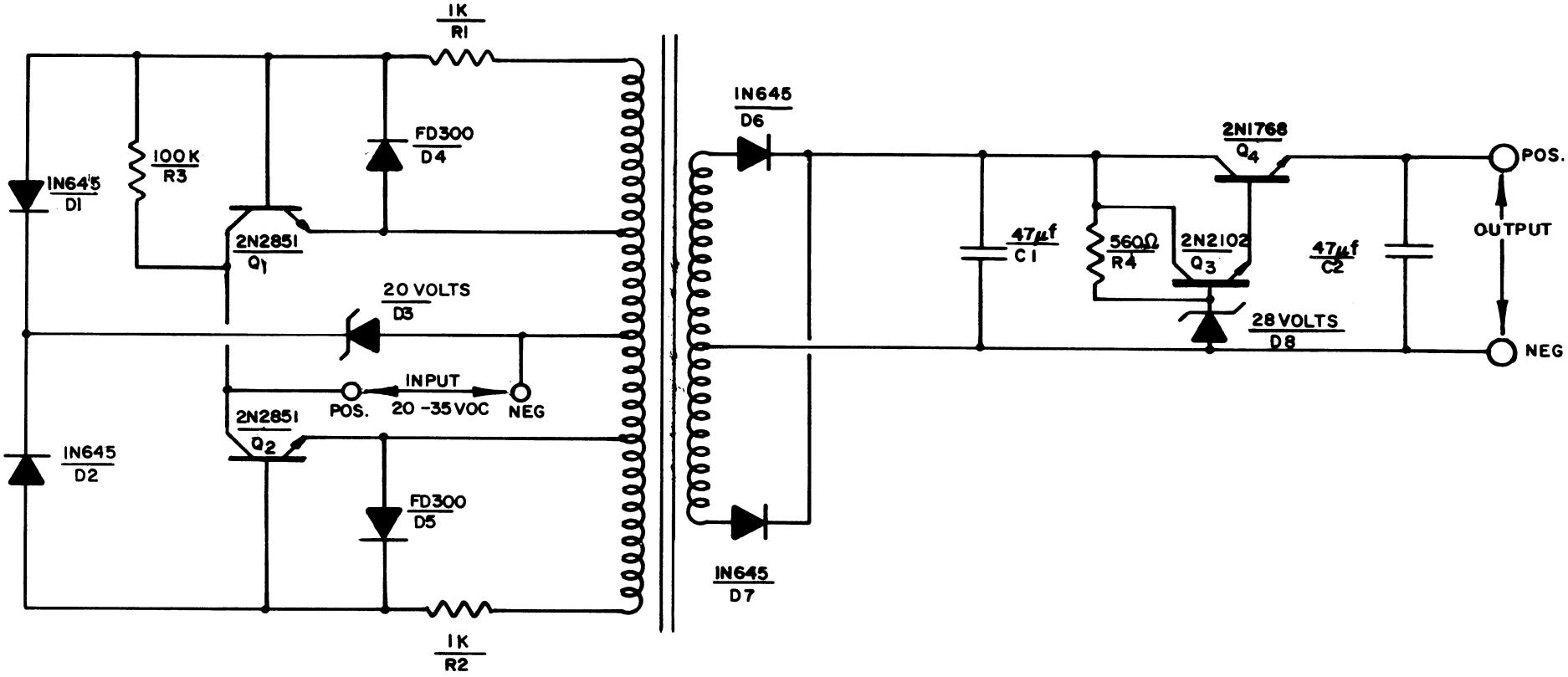

Figure 9. DC-DC converter power supply.

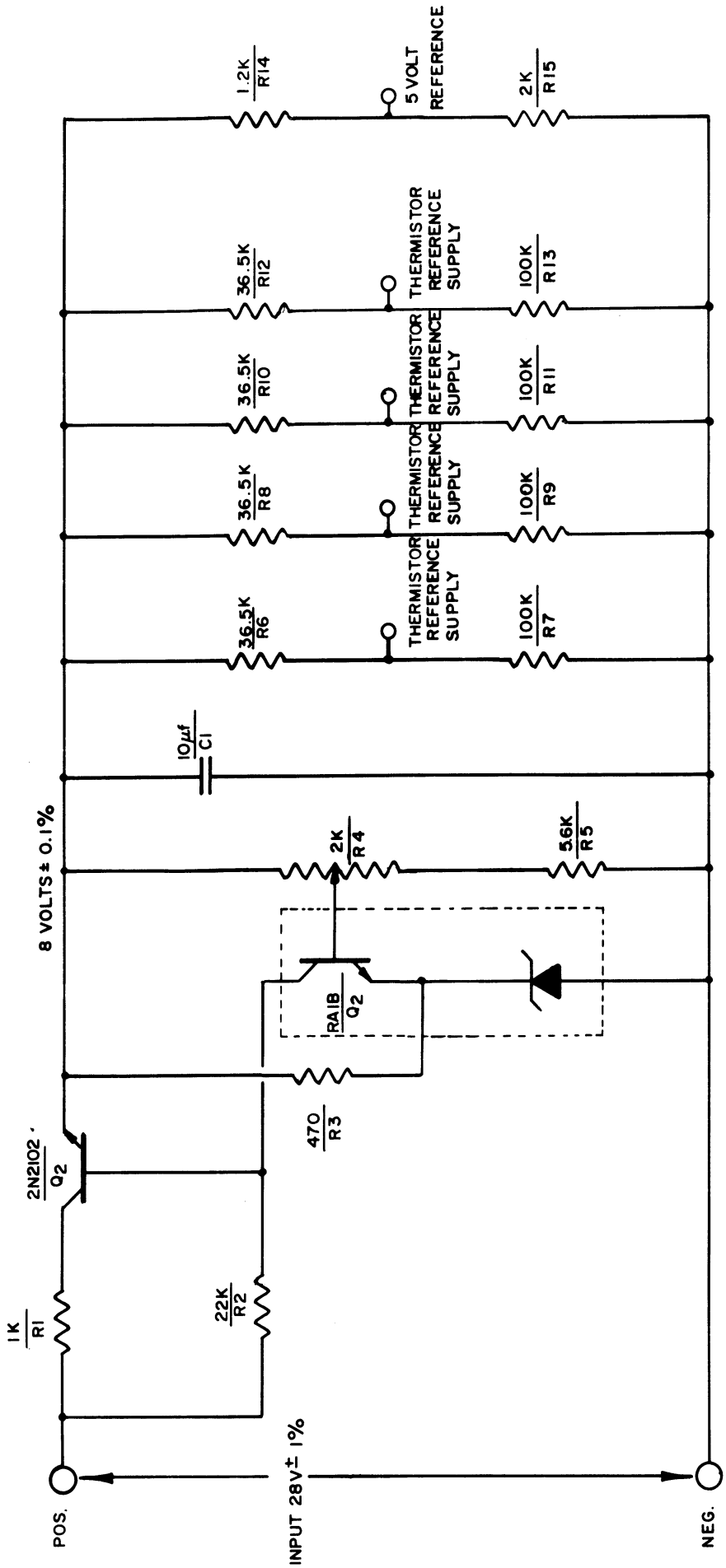

Figure 10. Thermistor and calibration supply circuit.

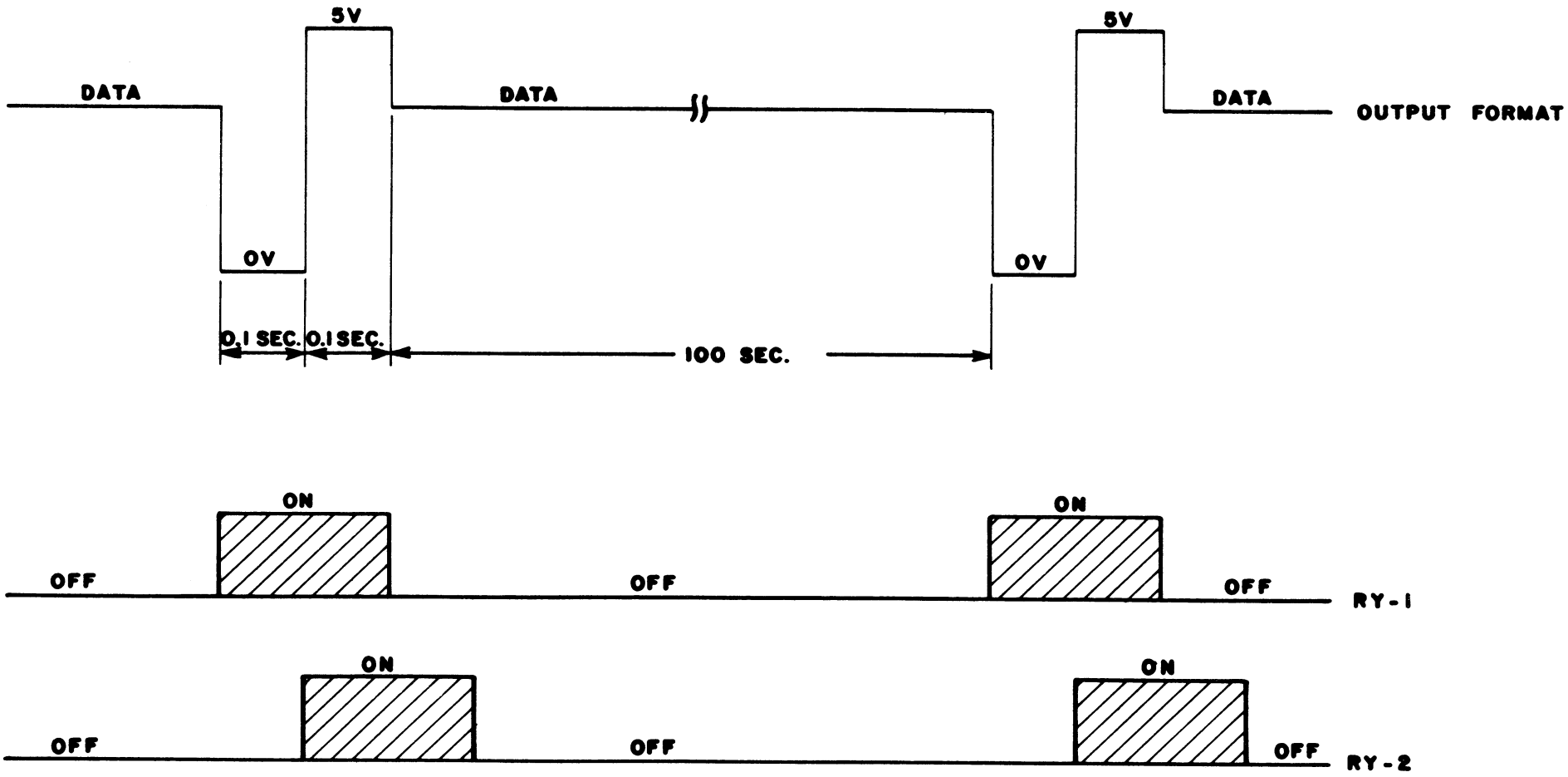

Figure 11. Calibration timer output format and relay switch timing.

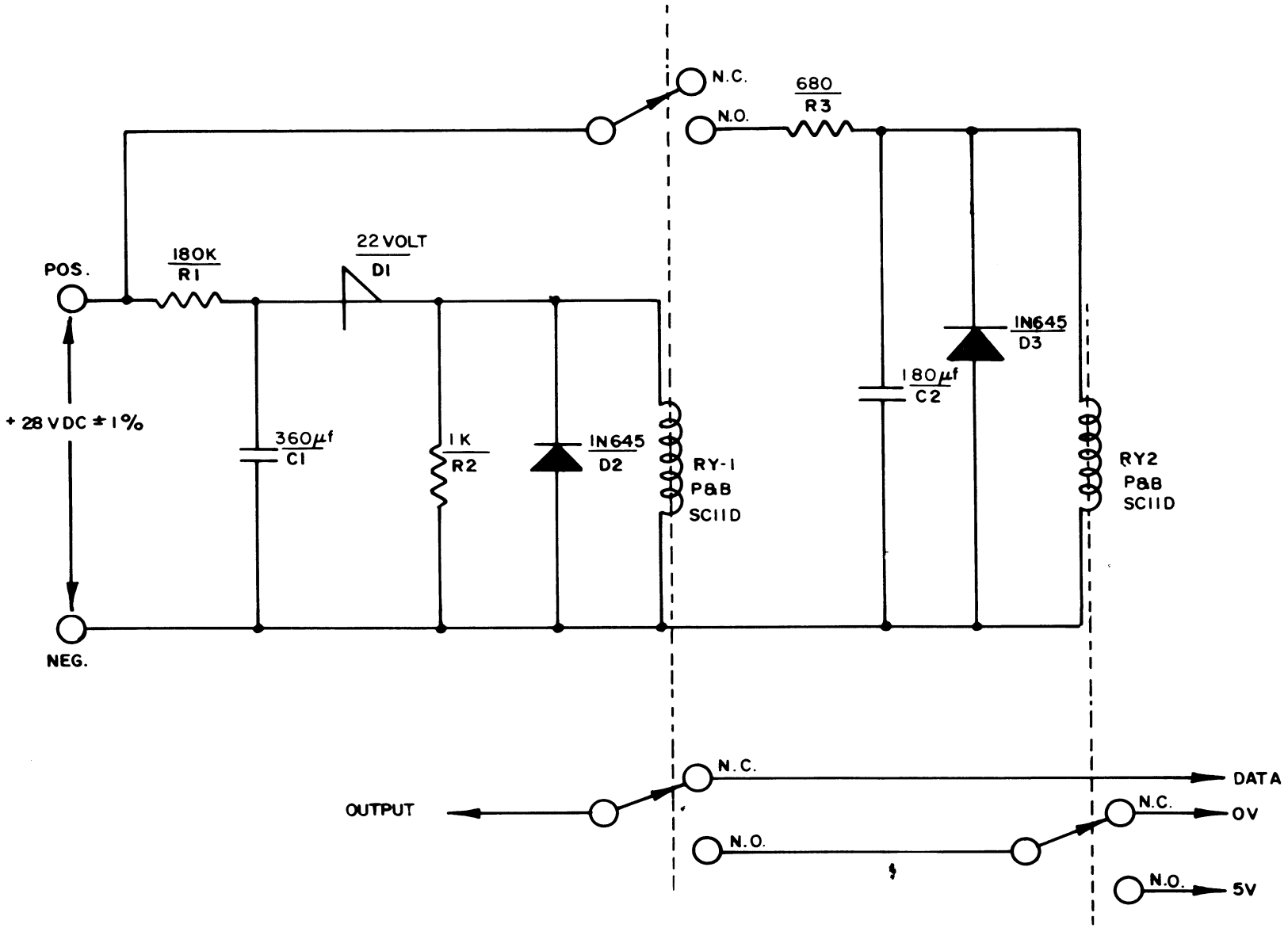

Figure 12. Calibration timer.

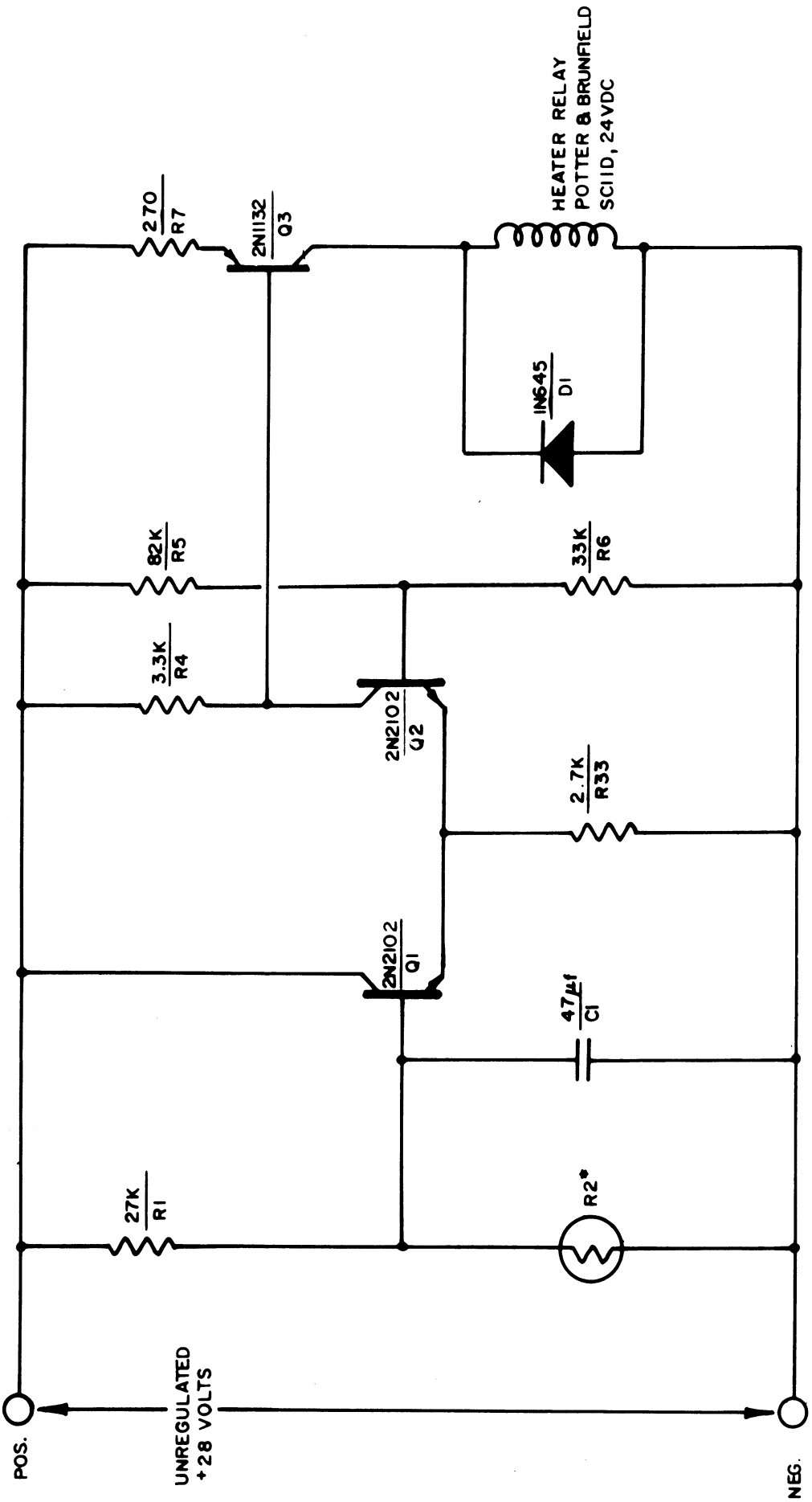

Figure 13. Heater control switching circuit.

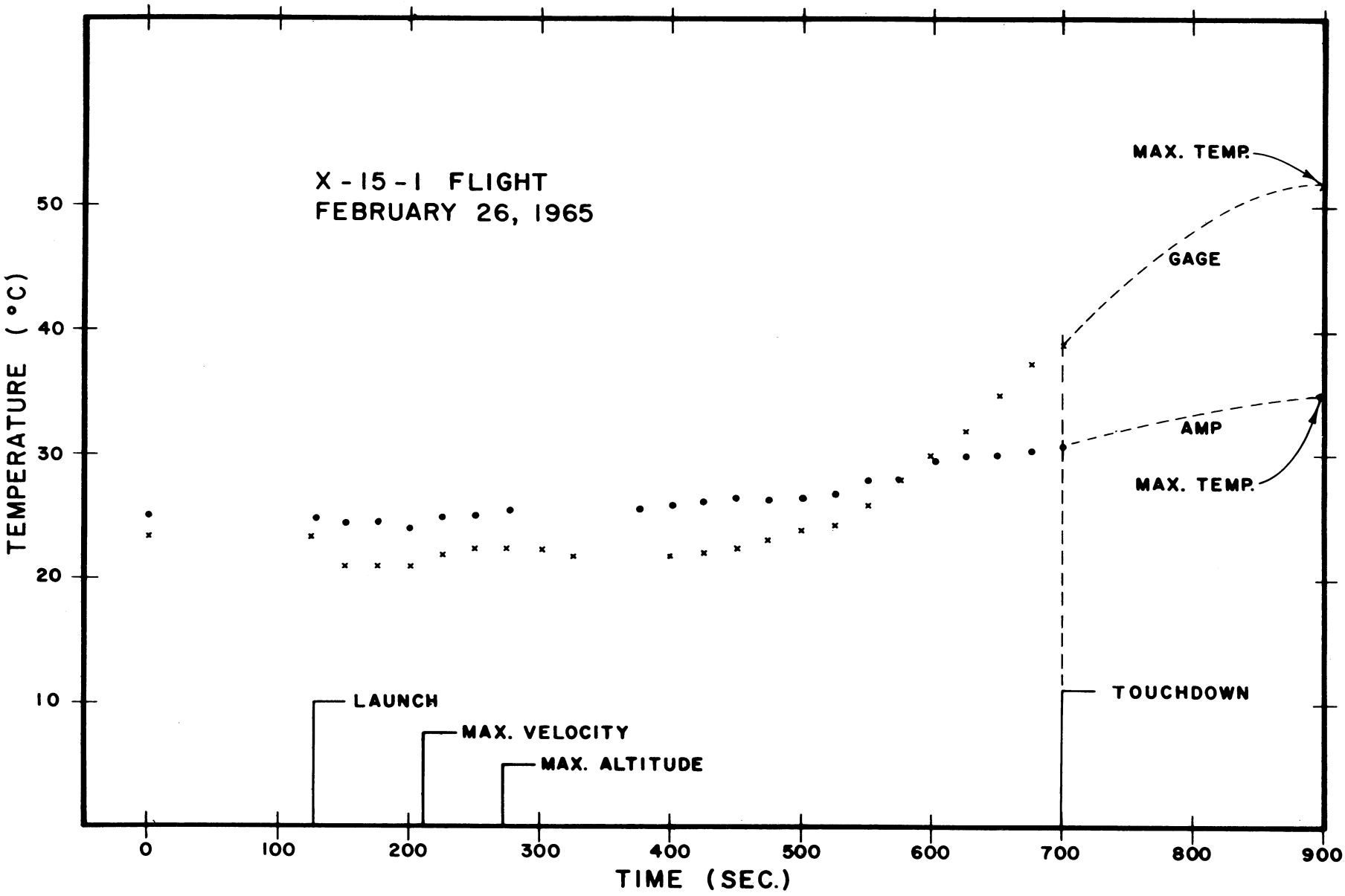

Figure 14. Gage and amplifier environmental temperature-time history, 26 February 1965.

4. MEASUREMENT TECHNIQUE

Measurement of the impact (pitot) pressure on a supersonic probe is an established technique for the determination of atmospheric ambient density profiles. Pitot measurements have been undertaken both on sounding rockets and ballistic vehicles (Saturn and Jupiter) as far back as 1946 when the first V-2 rockets became available as research tools. Atmospheric densities can be obtained from impact pressure data in the continuum-flow region by using a modified form of the Rayleigh pitot tube equation (Horvath, et al., 1962; Simmons, 1964),

$$\rho_a = \frac{P_i}{K(\gamma,M)V^2} \tag{4.1}$$

where ρ_a is the ambient density, P_i is the measured impact pressure, V is the free stream velocity, and $K(\gamma,M)$ is a function normally evaluated as a constant over the Mach number range resulting from a sounding rocket flight or, in this case, from an X-15 flight. Reduction of the measured impact pressure to an ambient density profile presupposes numerous idealized conditions. Some of the more important parameters are undisturbed free stream probe environment, contamination, velocity profile, position (altitude) profile, atmospheric winds, angle of attack, gage response, gage calibration, and display of gage output. Evaluation of these possible sources of error, at least in the continuum-flow region, is rather straightforward for sounding rocket-borne pitot probes. Analysis of the pitot data from the third and fifth flights points out the severity of the X-15 environment affecting the impact pressure measurement.

4.1. UNDISTURBED FREE STREAM PROBE ENVIRONMENT

The plan view of the pitot probe position is shown in Figure 15. The bow shock wave angle, Φ, is a function of the free stream Mach number, and the effective semi-vertex angle is determined by the nose of the X-15 aircraft. Discontinuities in the indicated impact pressure for the ascent and the descent portions of the flight profile show that a Mach number of at least 3.5 is required before the pitot orifice is forward of the bow shock. The magnitude of the pressure change is approximately 15 percent of the indicated pressure value. The altitude where the transition takes place is 30 km and can probably be considered a typical altitude of occurrence for a high altitude flight.

4.2. ERRORS DUE TO CONTAMINATION

There are two major sources of contamination which can influence the pitot

measurement for the configuration adapted on the X-15 aircraft, namely, the effects relative to the B-52 environment and the effects due to the environment of the X-15 itself during the launch phase.

4.2.1. B-52 Environment

In the prelaunch condition the X-15 was attached to the B-52 under its right wing and between the B-52 fuselage and the inboard engine nacelle (Figure 16). The proximity of the X-15 right wing pod to the B-52 engine exhaust presented the possibility of contaminants associated with the engine combustion products entering the exposed pitot orifice. Contamination inside the radioactive ionization gage chamber caused by engine exhaust could have caused an electrical leakage problem across the input terminals of the high impedance electrometer amplifier used for sensing the ionization gage current. Contamination inside the gage chamber could also increase the effective measured gage pressure, depending on the vapor pressure (and quantity) of the contamination constituents. Postflight inspections of the ionization gage chamber and antechamber did not reveal visual evidence of contaminants. Postflight calibration of the radioactive source also gave negative results, although the calibration took place several weeks after the actual X-15 flight and was therefore not a reliable indicator. The actual amplifier output data taken from the flight record provided the best source of information about prelaunch contamination. The design of the ionization gage for the altitude range up to and including 80 km was based upon the expected X-15 velocity and ambient density profiles. The 1 November 1966 flight reached an altitude of nearly 94 km, effectively placing the sensor in a zero pressure environment. The background or zero current reading of the ionization gage amplifier at the maximum altitude clearly showed a negligible constant biasing effect due either to electrical leakage or to outgassing.

4.2.2. X-15 Environment

Regulation of the roll, pitch, and yaw of the X-15 below 30 km is achieved in the conventional way by the control surfaces of the aircraft. Regulation of the vehicle attitude above 30 km requires the application of a reaction control system. This reaction or ballistic control system employs several strategically located rocket motors powered by hydrogen peroxide (Figure 17). Operation of these small rocket motors can affect the pitot measurement.

For the 1 November 1966 flight the reaction control motors were activated for 251.7 sec. During this time the six motors were energized 165 times with an average pulse time of 0.605 sec. The effects of the pulsed reaction motors were unique to three altitude zones, 30-50 km, 50-73 km, and above 73 km. Below 50 km there were no indicated effects in the impact pressure, even though five of the six reaction motors were energized at least once during the time the X-15 was in that region.

At 50 km, during the time when the number 3 reaction motor was energized, an abrupt impact pressure jump occurred. Thereafter, and until the X-15 reached 73 km, impact pressure jumps were noted each time motors 2 and 3 were pulsed. Response time of the impact pressure change to the reaction motor function was estimated to be less than 20 msec. No effects from motors 4, 5, and 6 were observed. Motor number 1 was not used in this altitude zone and therefore its effect could not be seen. The magnitude of the observed pressure changes was about 35 percent.

Above 73 km the effects of the reaction motors were continuous and irregular, indicating that residue from the hydrogen peroxide, probably water, had contaminated the inside of the ionization gage. The transition at 73 km was as abrupt as the one occurring at 50 km. As the vehicle reached apogee (94 km), the background pressure subsided. Pressure disturbances on reentry of the X-15 followed a pattern coincident with that described above.

The pressure jumps associated with on-off sequences of the two reaction motors (2 and 3) are not unlike those relating to the bow shock and are a clue to a possible mechanism explaining this behavior. As noted earlier, the bow shock crosses behind the wing pod orifice at Mach numbers greater than 3.5 (Figure 18a). Since the bow shock angle is a function only of Mach number and the effective semi-vertex angle of the bow of the X-15, the shock wave should remain behind the pitot orifice until the Mach number becomes less than 3.5, near the end of the flight. However, when the bow reaction motors are energized (1, 2, 3, or 4), the resulting pressure wave will intersect with the bow shock and, depending upon the relative shock strengths and pressure fields, will change the bow shock angle. Figure 18b indicates the probable flow condition in the region below 50 km. The shock lines A and B enclose the slip line or mass boundary (Shapiro, 1953). All of the lines remain behind the pitot orifice while a reaction motor is energized, and no impact pressure perturbation is observed. Flow fields 1 and 2 are required to have the same pressure. In order to maintain the pressure equivalence at lower atmospheric densities (pressures), the shock lines and mass boundary line must move outward. At 50 km shock line A crosses the pitot orifice with a resulting pressure jump (Figure 18c). The slip line, or mass boundary line, remains inside the orifice and prevents contamination from entering directly into the gage orifice. At 73 km the ambient density has decreased so that the mass boundary line (Figure 18d) has now passed over the pitot stagnation point. The amount of contamination deposited by the reaction motors directly into the gage depends upon the diffusion rate.

4.3. OTHER POSSIBLE SOURCES OF ERROR

4.3.1. Trajectory

Velocity and altitude of the X-15 are determined from three AFMTC-Mod II

radars (modified SCR-584 radars). There is no specific error analysis available for the reduced radar trajectories (Figure 19). Larson and Montoya (1964) estimated velocity errors of 2.6 percent, 3.75 percent, and 1.3 percent at 30.5 km, 45.6 km, and 61 km, respectively, for trajectories similar to those of the 1 November 1966 flight described here. The X-15 motor does not burn out until approximately 50 km, and thus provides the radars with an accelerating target until that time. As a result, the error estimates given above are more likely to be lower boundary conditions. On the assumption that they are of the proper order of magnitude, the density error will be twice the velocity error according to Equation (4.1).

A maximum altitude error estimate, also given by Larson and Montoya (1964), is 0.3 km. An atmosphere that is in hydrostatic equilibrium can be represented by the equation

$$\rho_2 = \rho_1 e^{-\frac{(h_2-h_1)}{H_\rho}} = \rho_1 e^{-\frac{\Delta h}{H_\rho}} \qquad (4.2)$$

where H_ρ = density scale height,
ρ_1 = density at h_1,
ρ_2 = density at h_2, and
Δh = estimated altitude error.

The density error resulting from an altitude error is a function of the scale height. An order-of-magnitude analysis can be made by choosing scale height values from the U.S. Standard Atmosphere, 1962. Appropriate limiting values are 8.05 and 5.4 for the stratopause and mesopause, respectively. Computation of the density error based on these values gives a range of 3.7 percent to 5.4 percent.

4.3.2. Angle of Attack

The angle of attack sensitivity for the pitot measurement can be estimated from a modified Rayleigh equation (Laurmann, 1958; Ainsworth, et al., 1961),

$$\rho \cong \frac{\frac{C_1 P_i}{\cos^{1/2}\alpha} - C_2 P_a}{V^2} \qquad (4.3)$$

where C_1, C_2 = known constants,
P_i = impact pressure,
P_a = ambient pressure, and
α = angle of attack.

The equation represents the results of wind tunnel tests and is applicable to the continuum flow region.

The radioactive ionization gage was designed to resolve impact pressures throughout the entire altitude range defined as the continuum region. An arbitrary altitude limit was set at 85 km beyond which viscosity correction factors and chamber geometry considerations would become important. A printout of the time-history of the X-15 angle of attack between 30 km and 85 km indicates a mean angle of attack of 4.17 deg with a standard deviation of $\pm$ 4.6 deg. The maximum angle of attack was 14.4 deg, occurring just before the X-15 motor burnout when increased angles were observed. Computation of the estimated error in the magnitude of the density, resulting from the indicated angles, gives a mean density error of 0.15 percent and a maximum error of approximately 1.5 percent.

4.3.3. Atmospheric Winds

Atmospheric winds can affect the pitot measurement by altering the effective velocity vector. The winds can change the magnitude of the velocity vector or the direction of the velocity vector or both. Atmospheric winds are considered to be mostly horizontal, a necessary condition for an atmosphere in hydrostatic equilibrium. The trajectory of most rocket-borne probes assumes near vertical elevation angles, that is, greater than 80 deg effective initial quadrant elevation (Q.E.). For the idealized case of a vertical trajectory (Q.E.=90 deg), a pure horizontal wind would effect only a direction change in the velocity vector, that is, angle of attack. A worst case of the order-of-magnitude analysis can be made to show the angle of attack sensitivity due to winds. Assume a vertical velocity vector of 1100 m/sec (the lowest velocity observed for an X-15 trajectory above 30 km) and a horizontal atmospheric wind of 100 m/sec. The vector angle change is

$$\Phi = \tan^{-1} \frac{W_H}{V} = \tan^{-1} \frac{100}{1100} = 5.5 \text{ deg} \qquad (4.4)$$

where W_H = horizontal wind velocity, and
V = vehicle velocity.

If the payload initially had a zero angle of attack, a 5.5 deg angle change in the effective velocity vector would induce a 0.25 percent error in the resultant density.

A vertical trajectory is, of course, unrealistic. The trajectory of a typical high altitude X-15 flight is ballistic; that is, the velocity vector never exceeds an elevation angle greater than 45 deg. Unless the plane of the flight path is normal to the horizontal wind component, magnitude changes in the effective velocity vector will occur. As an example, assume the X-15 to be moving at 1100 m/sec in an easterly direction with a Q.E. of 45 deg and zero angle of attack. Also assume a horizontal wind to be directly from the east at 100 m/sec. Both the wind and the vehicle vectors lie in the same plane with the component of the horizontal wind adding 70.7 m/sec to the inertial

velocity vector. The resulting error in density due to this wind factor amounts to twice the error in the effective velocity as shown in Equation (4.1).

$$\text{Density error} = \frac{2(70.7)}{1100}\ 100 = 12.8 \text{ percent.}$$

The error in angle of attack caused by the horizontal wind in this case has been neglected because it is at least an order of magnitude less.

During most periods of the year, atmospheric wind fields are zonal, westerly during the winter months and easterly during the summer. The meridional winds (north and south) are typically 10-20 m/sec. These conditions hold very well below an altitude of 70 km. Because of the predictable behavior of these winds, vehicle flight paths can be selected which best suit the measurement goal. Obviously, a north-south azimuth is preferable.

The 1 November 1966 X-15 flight had a flight path which was less than 6.0 deg from a true meridional direction (Figure 20). Atmospheric wind data taken to an altitude of approximately 55 km at Point Mugu, California, on 2 November, 3 November, and 4 November 1966 all confirm meridional winds of less than 10 m/sec. The zonal winds are equally consistent, increasing linearly from zero m/sec at 25 km to 60 m/sec at 55 km. The estimated maximum density error due to horizontal atmospheric winds for the 1 November 1966 flight is less than 1 percent.

4.3.4. Gage and Amplifier Response

Location of the gage chamber, antechamber, and amplifier is shown in Figure 21. The response of the sensor system to impact pressure changes was measured, inadvertently, when the reaction motors influenced the impact pressure in the step-function manner described in Section 4.2.2. Figure 22 illustrates, in the real time oscillograph recording, the response of the gage output for three discrete motor functions. Timing line divisions are in increments of 0.1 sec. The estimated response time is observed to be less than 20 msec.

4.3.5. Calibration of the Gage

The sensor used for the 1 November 1966 pitot measurement on the X-15 aircraft is a radioactive ionization gage (El-Moslimany, 1960). The radioactive gage when combined with a multirange electrometer amplifier, as used here, is referred to as a densatron. An ionization gage can be designed to suit the unique pressure (density) environment. The gage used on the X-15 has a linear ionization current-pressure relationship with a sensitivity of 10^{-10} A/torr. Its linear pressure range covered 0.1 torr to 125 torr, equivalent to an altitude range of between 30 and 80 km for an X-15 flight. The mean deviation of the linear current-pressure relationship is +0.5 percent with a standard

deviation of less than 1 percent. These numbers were obtained by using 36 unsmoothed calibration points over the indicated pressure range.

The ionizing agent used in the gage for 1 November 1966 is Americium 241 (Am241), an alpha emitter with an energy of 5.5 MeV and a half-life of 470 years. Decay of the radioactive source follows the disintegration law

$$N(t) = N_o e^{-\lambda t} \tag{4.5}$$

where λ, the disintegration constant for Am 241, is 0.001475/year. A simple calculation shows that it requires 6.8 years to reduce the activity 1 percent. The above characteristics of Am 241 qualify it as a stable ionizing agent.

Repeatability of calibration in the indicated pressure range is accurate to better than 1 percent. The accuracy of the calibration depends upon the reference standards used. The several standards used redundantly to obtain maximum accuracy are the following:

1. Three Wallace & Tiernan manometers (0-20 torr, 0-100 torr, and 0-760 torr),

2. A McLeod mercury manometer,

3. An incremental volume input system (Flanick and Ainsworth, 1961), and

4. Laboratory mounted radioactive ionization gages.

The absolute accuracy of the final gage calibration is estimated to be better than 3 percent throughout the entire pressure range, 0.1 to 125 torr.

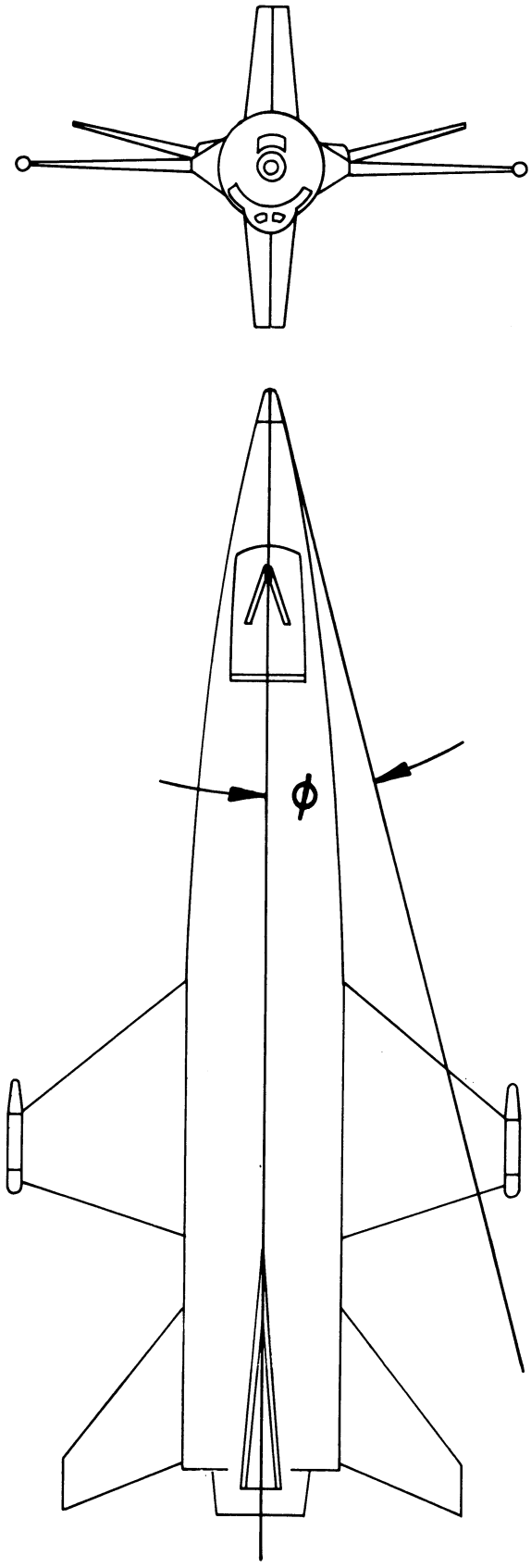

Figure 15. Typical bow shock angle above 30 km.

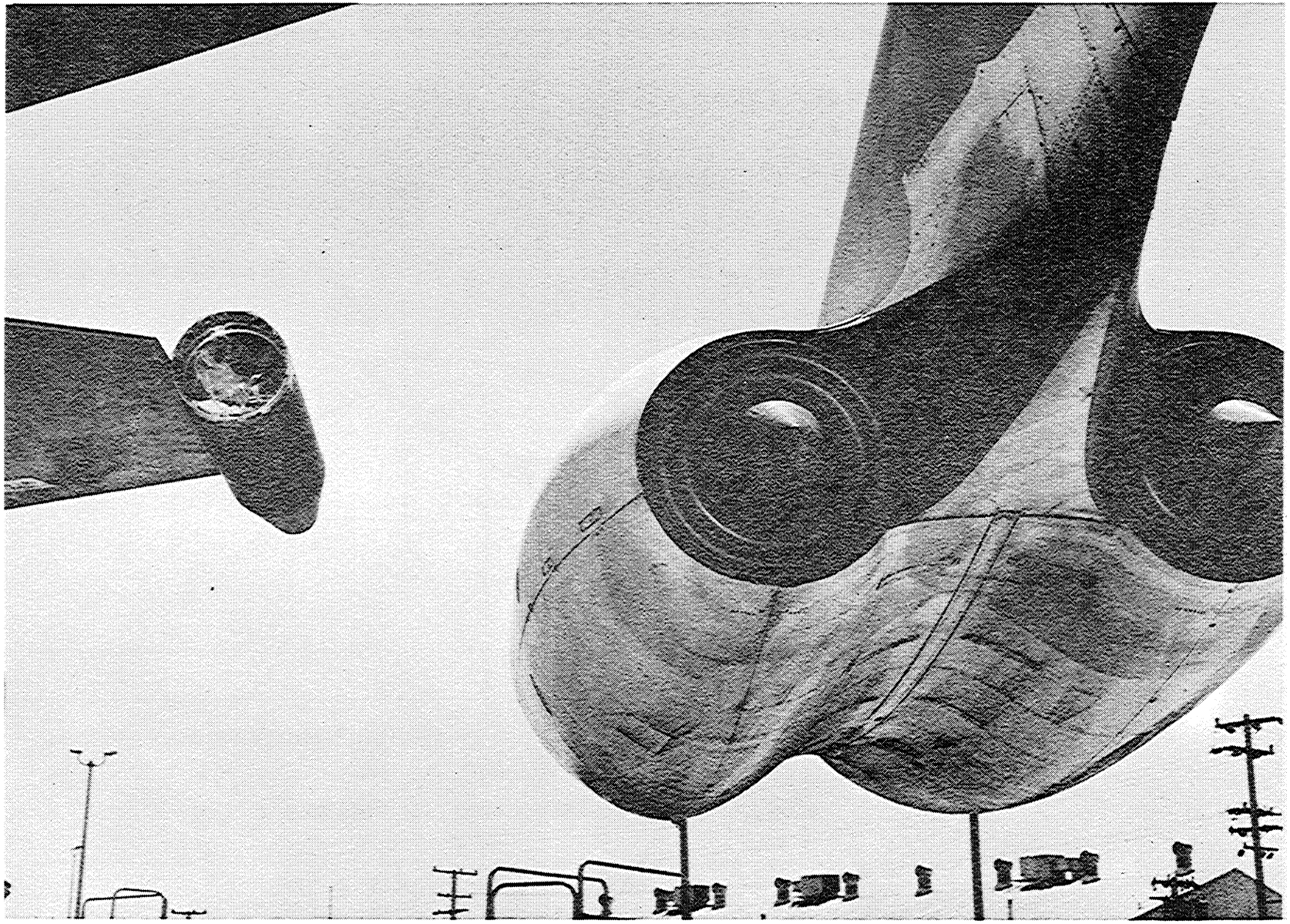

Figure 16. The X-15 wing pod and B-52 engine nacelle.

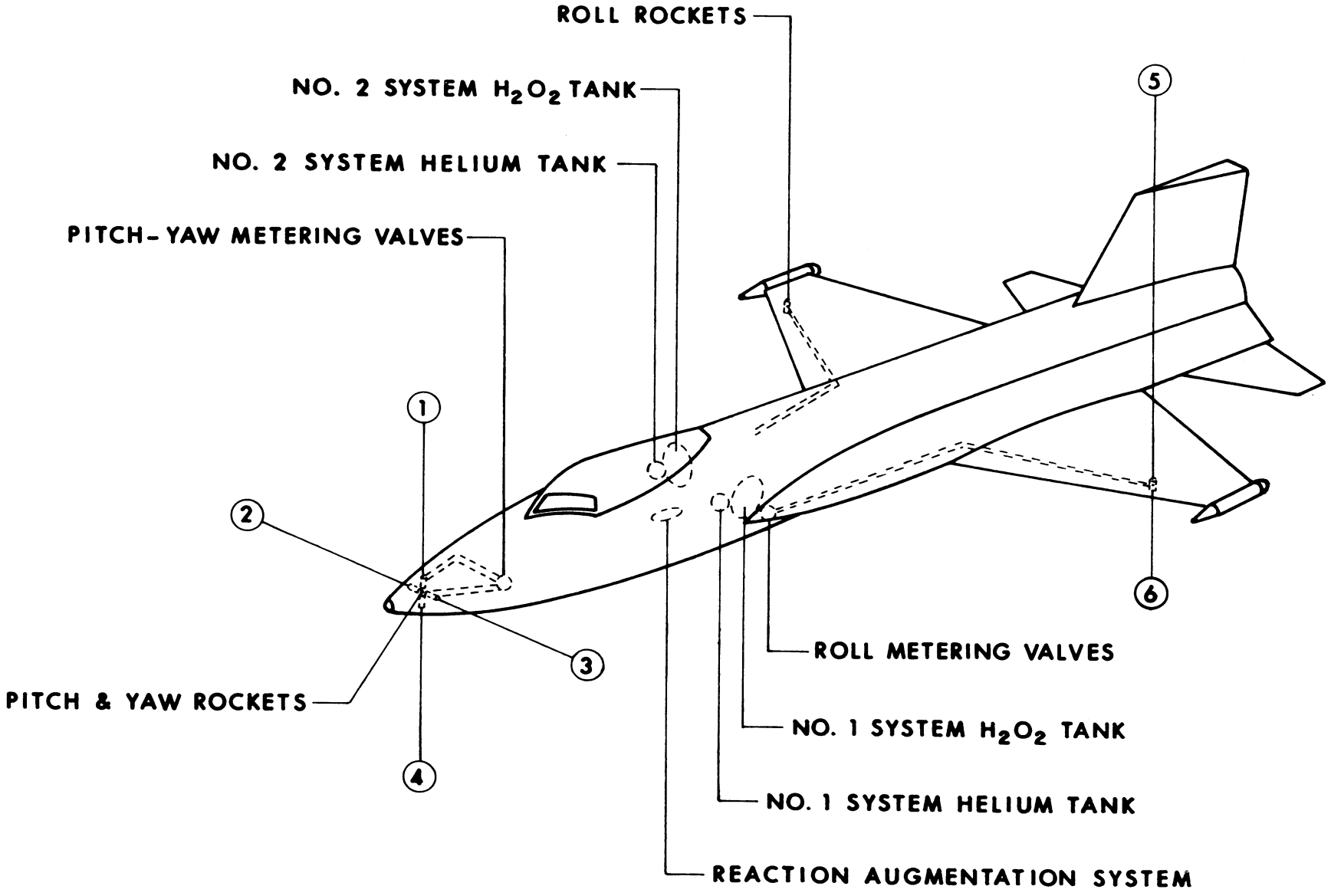

Figure 17. Location of reaction control system components in X-15.

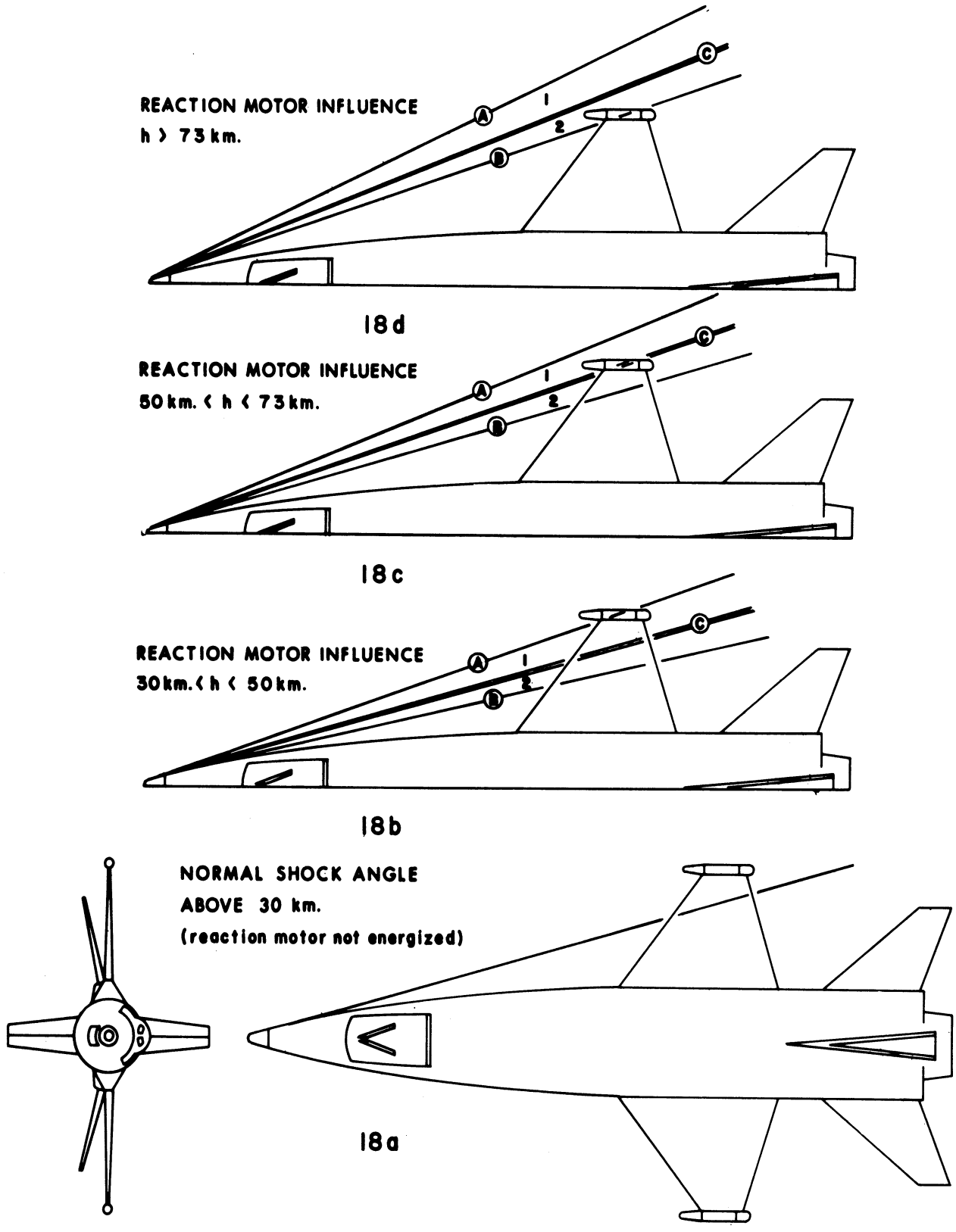

Figure 18. Reaction motor influence on the bow shock angle.

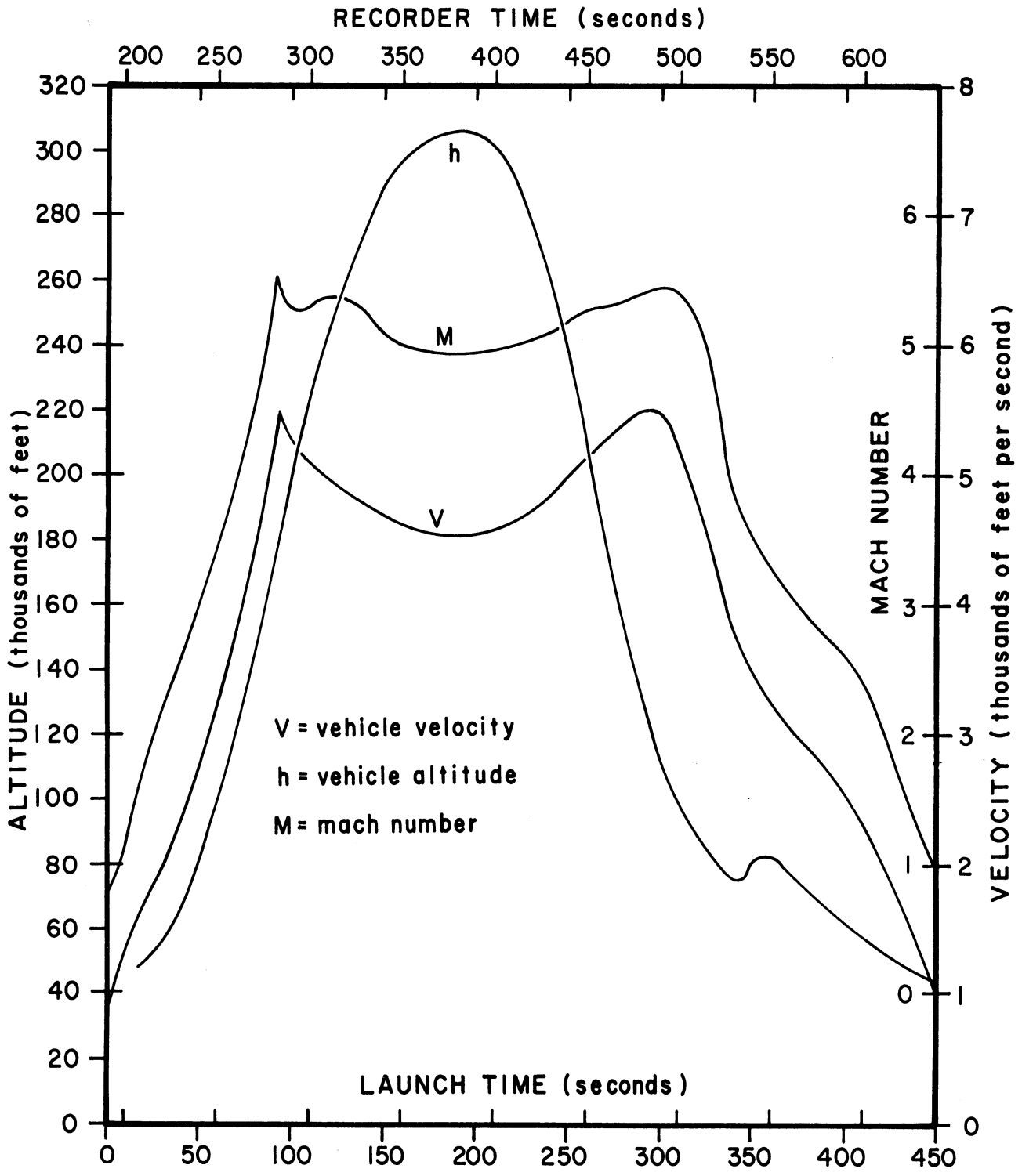

Figure 19. Typical X-15 launch time trajectory parameters.

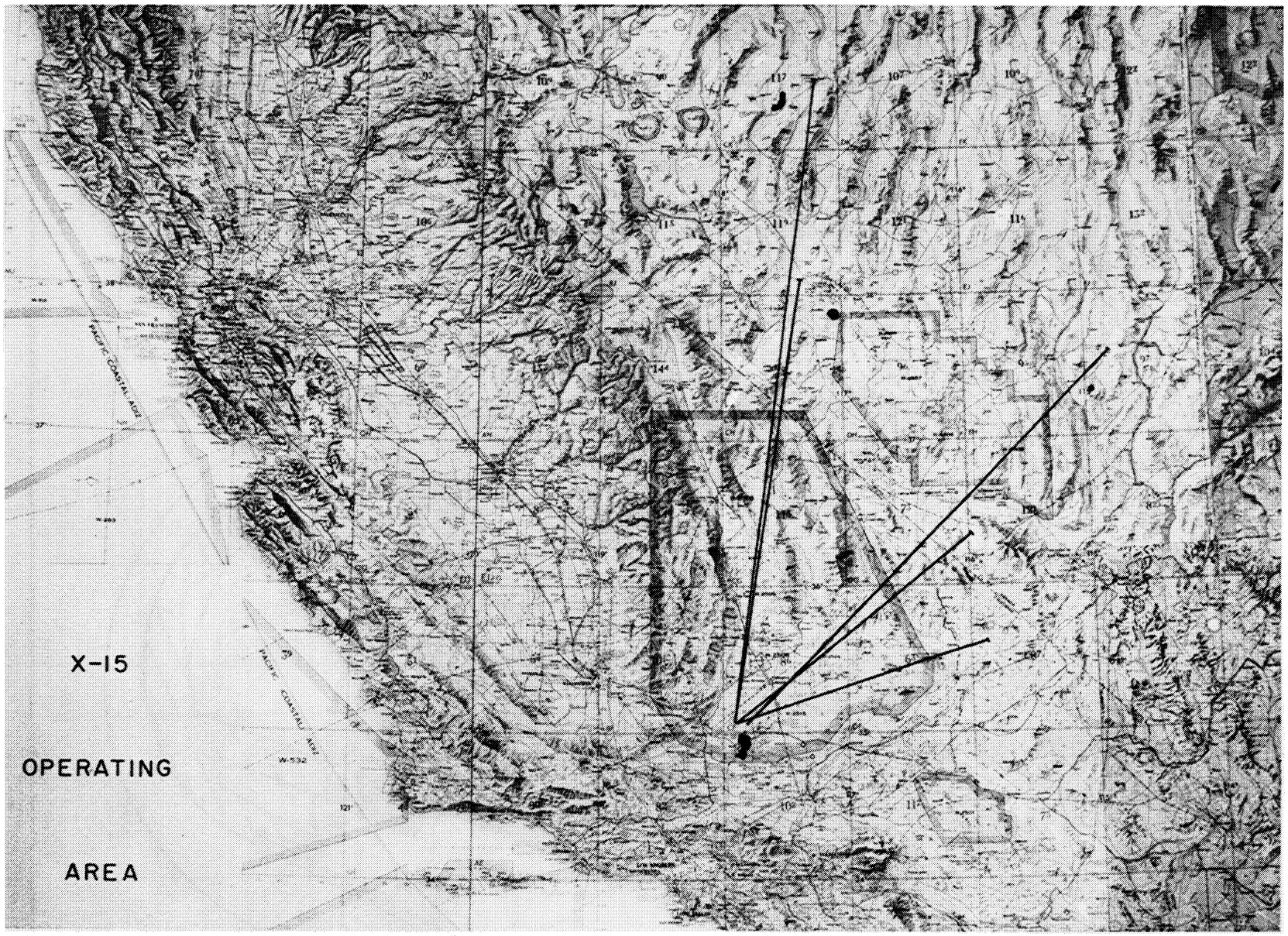

Figure 20. The X-15 operating area.

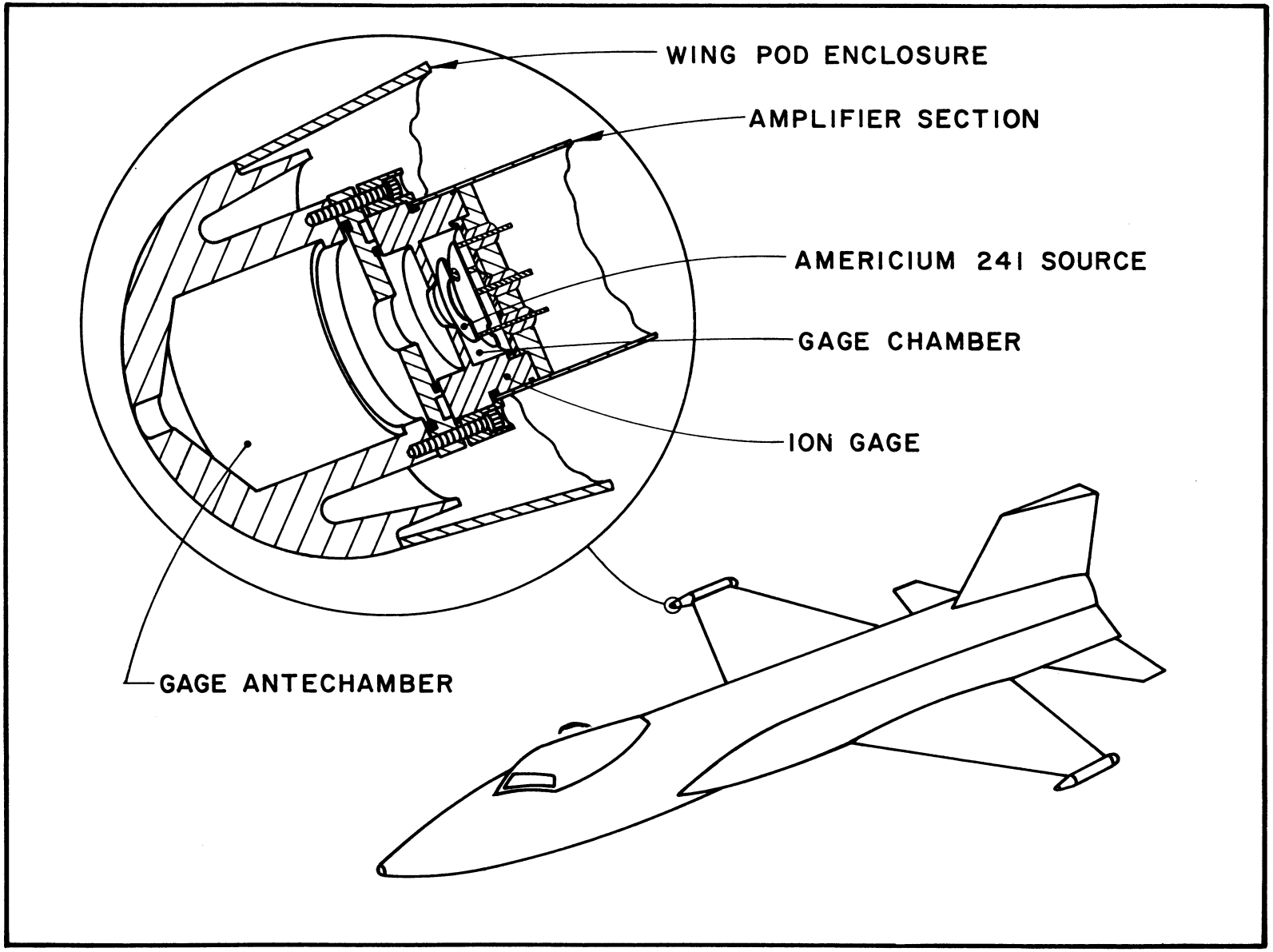

Figure 21. Impact pressure sensor and amplifier location.

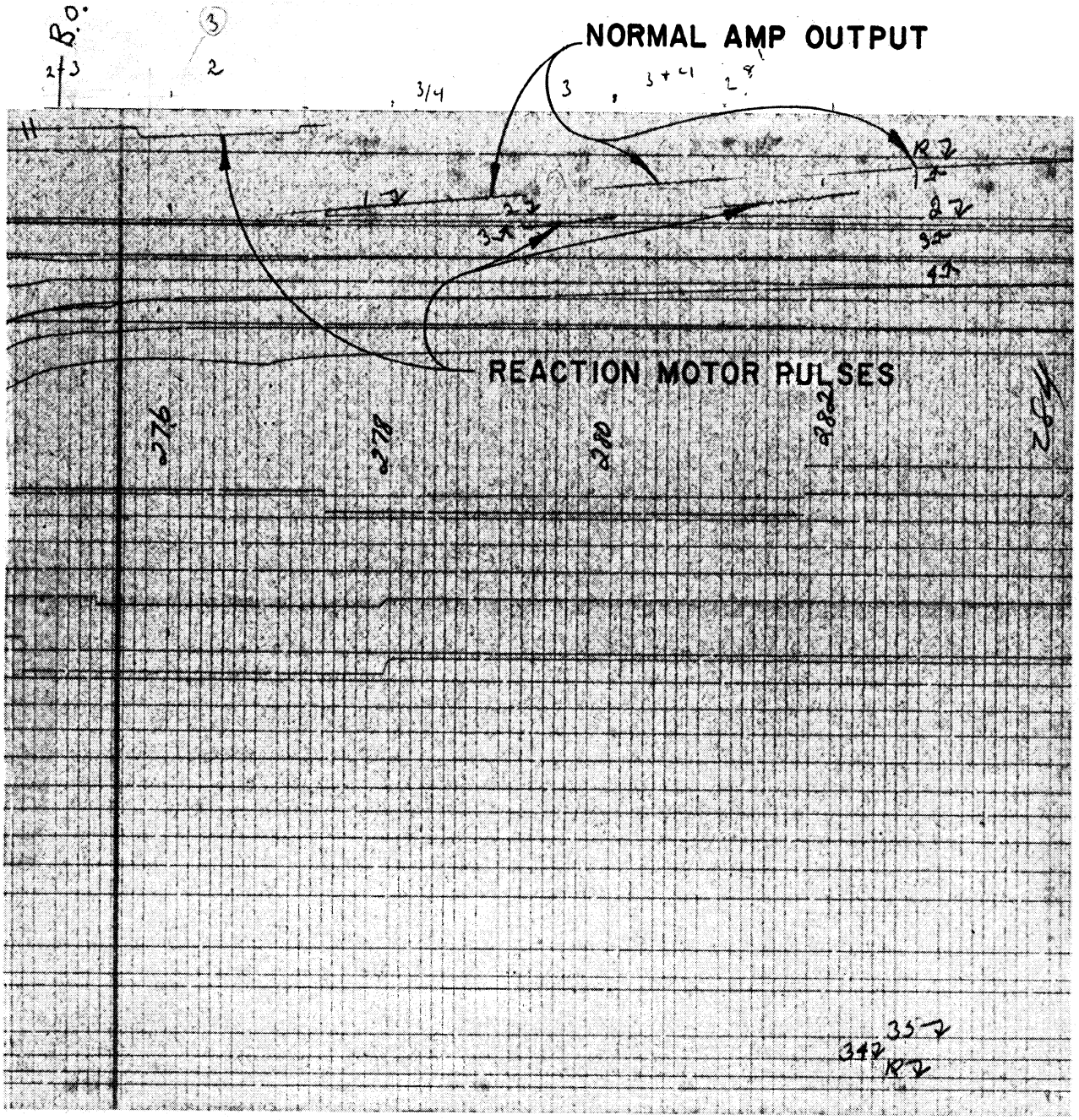

Figure 22. Gage output response.

5. DISCUSSION

The X-15 with its wing pod instrumentation modification seemed to be an ideal vehicle for carrying pitot measuring devices into the upper atmosphere on a regular basis. However, the anticipated regularity of X-15 flights never materialized. A total of five pitot-instrumented flights took place during the four-year research effort. Consequently, concentrated research activity was severely limited.

The pitot measurements from the 1 November 1966 flight, the last and most successful of five launches, yielded the data for the ambient density profile shown in Figure 3. At first glance, the profile appears to be reasonable and is accurate with regard to order of magnitude. Analysis of the X-15 environment, however, pointedly shows several conditions unique to the X-15 which give good reason to question the absolute accuracy of the measurement.

The 1 November 1966 flight reached an altitude of 93.5 km. During transit between launch and apogee, the pitot measurement was influenced by the X-15 environment in four continuous altitude increments. Below 30 km the pitot orifice on the wing pod lies behind the bow shock wave. A pressure distribution, a function of the bow shock angle which in turn is a function of the Mach number for the X-15 configuration, exists in this region. The ideal pitot measurement can be in error as much as 15 percent due solely to the bow shock interference.

The second altitude increment, 30-50 km, is extremely critical because the X-15 engine, still operating, presents the radar trackers with an accelerating target. The large perturbation in the density deviation profile near the 50 km level is indicative of the trajectory errors. It is not possible to assign and exact magnitude to the error in the density measurement because of the inconsistent trajectory data. However, the engine burns out at 50 km, and at this altitude, trajectory errors appear to influence the density measurement by an estimated 20 percent (Figure 3).

The pitot measurement is again affected by the bow shock in the region from 50-73 km. The small rocket motors used for attitude control emit a pressure wave which interacts with the bow shock. This interaction causes the shock angle, Φ, to increase whenever the interfering attitude control motor is energized. The increased shock angle creates a situation almost identical with that occurring below 30 km; however, this condition occurs only during the times when a disturbing rocket motor is operating. An estimated 20 percent of the pitot data in this altitude region was lost because of the influence of the attitude rocket motors. Uncertainty in the trajectory, just after engine burnout, above 50 km, is an additional source of error in this altitude increment. The estimated maximum error in density caused by the erroneous tra-

jectory is 20 percent at 50 km. The error decreases to the probable error given by Larson and Montoya (1964) of less than 3 percent at 60 km.

Above 73 km, the fourth region, the bow shock angle was affected by the attitude control motors to such an extent that the shock angle permitted residue, probably water, for the hydrogen-peroxide powered control motors to enter the pitot orifice chamber. The contamination resulted in an incoherent amplifier output with a consequent lack of pitot data above 73 km.

The conclusion reached on the basis of information gathered during this research effort is that the most serious error affecting the X-15 density data is in the X-15 trajectory, particularly in the velocity profile. The entire density profile is limited on the low altitude end (approximately 30 km) by the bow shock interference and on the high altitude end (approximately 73 km) by the residue from the reaction control motors. In the region from 50 to 73 km the reaction control motor intermittently biases the gage output, but sufficient information is available for data analysis. Without the inaccurate velocity and possibly altitude parameters, the X-15, using the present wing pod configuration, can yield density profiles between the altitudes of 30 and 73 km.

6. BIBLIOGRAPHY

Ainsworth, J. E., Fox, D. F., and Lagow, H. E., "Upper Atmosphere Structure Measurement Made with the Pitot-Static Tube," Journal of Geophysical Research, 66, No. 10, 3191-3212, 1961.

Ames Research Staff, Equations, Tables, and Charts for Compressible Flow, National Advisory Committee for Aeronautics, Report No. 1135, 1953.

Flanick, A. P., and Ainsworth, J. E., "Vacuum Gauge Calibration System (10^{-2} to 10^{1} mmHg)," Review of Scientific Instruments, 32, No. 4, 408-410, April 1961.

Hines, P. B., Dovap Systems and Data Reduction Methods, New Mexico State University, Physical Science Laboratory, University Park, New Mexico, January 1962.

Horvath, J. J., Simmons, R. W., and Brace, L. H., Theory and Implementation of the Pitot-Static Technique for Upper Atmosphere Measurements, University of Michigan Scientific Report 04673-1-S, March 1962.

Larson, T. L., and Montoya, E. J., "Stratosphere and Mesosphere Densities Measured with the X-15 Airplane," Journal of Geophysical Research, 69, No. 24, 5123-5130, December 1964.

Laurmann, J. A., Low Density Characteristics of an Aerobee-Hi Pitot-Static Probe, University of California, Institute of Engineering Research, Technical Report HE-150-156, May 1958.

El-Moslimany, M. A., Theoretical and Experimental Investigation of Radioactive Ionization Gauges, University of Michigan Scientific Report 03554-4-S, May 1960.

Murgatroyd, R. J., "Winds and Temperatures Between 20 km and 100 km—A Review," Quarterly Journal of the Royal Meteorological Society, 83, No. 358, 417-454, October 1957.

Nagy, A. F., Spencer, N. W., Niemann, H. B., and Carignan, G. R., Measurement of Atmospheric Pressure, Temperature, and Density at Very High Altitudes, University of Michigan Final Scientific Report 02804-7-F, August 1961.

Newell, H. E., High Altitude Rocket Research, Academic Press, New York, 1953.

Rupert, G. F., Engineering Design of a Pitot-Static Probe Payload, University of Michigan Engineering Report 05776-2-E, April 1967.

Schultz, F. V., Spencer, N. W., and Reifman, A., Atmospheric Pressure and Temperature Measurements Between the Altitudes of 40 and 100 Kilometers, Upper Atmosphere Report No. 2, University of Michigan Research Institute, Ann Arbor, July 1948.

Shapiro, A. H., Dynamics and Thermodynamics of Compressible Fluid Flow, 1, The Ronald Press, New York, 1953.

Sherman, F. S., New Experiments on Impact Pressure Interpretation in Supersonic and Subsonic Rarefied Airstreams, NACA Technical Note 2995, September 1953.

Simmons, R. P., An Introduction to the Theory and Data Reduction Method for the Pitot-Static Technique of Upper Atmosphere Measurement, University of Michigan Scientific Report 05776-1-S, March 1964.

U. S. Standard Atmosphere, 1962, U.S. Government Printing Office, Washington, D.C., December 1962.

CRL CONTRACTOR DISTRIBUTION LIST

AFCRL (CRMXLR) Stop 29
L. G. Hanscom Field
Bedford, Massachusetts 01730
5 Copies

AFCRL (CRMXRA) Stop 39
L. G. Hanscom Field
Bedford, Massachusetts 01730
10 Copies

Please attach the Notice of Distribution Completed to the copy addressed to :

AFCRL (CRMXRP) - Stop 30
L. G. Hanscom Field
Bedford, Massachusetts 01730

AFCRL (CRN) Stop 30
L. G. Hanscom Field
Bedford, Massachusetts 01730

AFCRL (CRTE) Stop 30
L. G. Hanscom Field
Bedford, Massachusetts 01730

AFCRL (CRTPM) Stop 30
L. G. Hanscom Field
Bedford, Massachusetts 01730

West Coast Office, AFCRL
Attn Mr. Gene M. DeGiacomo
SMT/CRZ
Los Angeles Air Force Station
Los Angeles, California 90045

ADC
Operations Analysis Office
Ent Air Force Base
Colorado 80912

AFAL (AVX)
Wright-Patterson AFB
Ohio 45433

Hq., AFCRL (CRES) Stop 30
Attn Gerard A. Faucher
L. G. Hanscom Field
Bedford, Massachusetts 01730
10 Copies

AFETR
Technical Library-MU-135
Patrick AFB, Florida 32925

AFIT (MCLI, Library)
Building 640 - Area B
Wright-Patterson AFB, Ohio 45433

AFSC-STLO (RSTAL)
AF Unit Post Office
Los Angeles, California 90045

AFSC-STLO (RTSAB)
Waltham Federal Center
424 Trapelo Road
Waltham, Massachusetts 02154

AFSC-STLO (RTSUM)
68 Albany Street
Cambridge, Massachusetts 02139

AFWL (WLIL)
Kirtland AFB, New Mexico 87117

Dir., Air University Library
Attn AUL3T
Maxwell AFB, Alabama 36112

APGC (PGBPS-12)
Eglin AFB, Florida 32542

OAR (RRY)
1400 Wilson Boulevard
Arlington, Virginia 22209

RADC (EMTLD)
Attn Documents Library
Griffiss AFB, New York 13440

RTD
Scientific Director
Bolling AFB, Washington D. C. 20332

FAA
Bureau of Research & Development
300 Independence Avenue, S. W.
Washington, D. C. 20553

SAC (OA)
Offutt AFB, Nebraska 68113

SSD (SSTRT)
Attn Lt. O'Brien
Los Angeles Air Force Station
AFUPO
Los Angeles, California 90045

Hq., TAC (OA)
Langley AFB, Virginia 23362

USAF Academy
Academy Library (DFSLB)
Colorado 80840

Army Missile Command
Attn Chief, Document Section
Redstone Scientific Info. Center
Redstone Arsenal, Alabama 35809

U. S. Army Electronics Command
Attn AMSEL-RD-MAT
Technical Document Center
Fort Monmouth, New Jersey 07703

U. S. Army Research Office
Attn Technical Library
3050 Columbia Pike
Arlington, Virginia 22204

Naval Ordnance Laboratory
Technical Library
White Oak, Silver Spring
Maryland 20910

Commanding Officer
Office of Naval Research Branch Off.
Box 39 - Fleet Post Office
New York 09510
2 Copies

Director
Naval Research Laboratory
Attn 2027
Washington, D. C. 20390

NASA-Lewis Research Center
Library - Mail Stop 60-3
21000 Brookpark Road
Cleveland, Ohio 44135

U. S. Naval Ordnance Test Station
Attn Technical Library
China Lake, California 93555

U. S. Naval Postgraduate School
Library (Code 2124)
Monterey, California 93940

U. S. Navy Electronics Laboratory
(Library)
San Diego, California 92152

Central Intelligence Agency
Attn OCR/DD/STD. Distribution
Washington, D. C. 20505

Clearinghouse for Federal Scientific
& Technical Information (CFSTI)
Sills Building
5285 Port Royal Road
Springfield, Virginia 22151

Director
Defense Atomic Support Agency
Washington, D. C. 20305
2 Copies

Document Receipt Notice Card Plus :

Defense Documentation Center (DDC)
Cameron Station
Alexandria, Virginia 22314
20 Copies

DIA
(DIAAP-142)
Washington, D. C. 20301

Environmental Sciences Services Adm.
Library
Boulder Laboratories
Boulder, Colorado 80302
2 Copies

Government Printing Office
Library
Division of Public Documents
Washington, D. C. 20402

Library of Congress
Aerospace Technical Division
Washington, D. C. 20540

Library of Congress
Exchange & Gift Division
Washington, D. C. 20540

NASA Scientific & Technical
Information Facility
Attn Acquisitions Branch (S-AK/DL)
P. O. Box 33
College Park, Maryland 20740

NASA-Flight Research Center
Library
P. O. Box 273
Edwards, California 93523

NASA-Goddard Inst. for Space Studies
(Library)
2880 Broadway
New York, New York 10025

NASA-Goddard Space Flight Center
Technical Library
Greenbelt, Maryland 20771

NASA-Jet Propulsion Laboratory
Attn Library (TDS)
4800 Oak Grove Drive
Pasadena, California 91103

Battelle Memorial Institute
Library
505 King Avenue
Columbus, Ohio 43201

The Mitre Corporation
Attn Library
P. O. Box 208
Bedford, Massachusetts 01730

The Rand Corporation
Attn Library-D
1700 Main Street
Santa Monica, California 90406

NASA-Manned Spacecraft Center
Technical Library
Houston, Texas 77058

National Center for Atmospheric
Research
NCAR Library, Acquisitions
Boulder, Colorado 80302

ODDR&E (Library)
Room 3C-128
The Pentagon
Washington, D. C. 20301

Reports with NOTICE NO. 1 only
to be sent to :

AIAA-TIS Library
750 Third Avenue
New York, New York 10017

Aerospace Corporation
Attn Library Acquisitions Group
P. O. Box 95085
Los Angeles, California 90045

British Defence Staffs
British Embassy
Scientific Information Officer
3100 Massachusetts Avenue, N. W.
Washington, D. C. 20008
3 Copies

Chief, Canadian Defence
Research Staff
2450 Massachusetts Avenue, N. W.
Washington, D. C. 20008
3 Copies

Technical & Scientific Reports
Will Be Released For Military
Purposes Only And Any Pro-
prietary Rights Which May Be
Involved Are Protected By
United States/United Kingdom
& Canadian Government Agree-
ments.

National Research Council
National Science Library
Ottawa,7 Canada

REMAINING COPIES TO BE RETAINED BY THE CONTRACTOR

Unclassified

Security Classification

DOCUMENT CONTROL DATA - R & D

(Security classification of title, body of abstract and indexing annotation must be entered when the overall report is classified)

1. ORIGINATING ACTIVITY (Corporate author)
The University of Michigan
Space Physics Research Laboratory, Department of Electrical Engineering, Ann Arbor, Michigan 48105

2a. REPORT SECURITY CLASSIFICATION
Unclassified

2b. GROUP

3. REPORT TITLE

PITOT MEASUREMENTS ON AN X-15 ROCKET PLANE

4. DESCRIPTIVE NOTES (Type of report and inclusive dates)
Scientific Final. Period covered: 1 October 1968 through 31 March 1968

5. AUTHOR(S) (First name, middle initial, last name)
Approved: 21 August 1968

Jack J. Horvath
Gary F. Rupert

6. REPORT DATE	7a. TOTAL NO. OF PAGES	7b. NO. OF REFS
August 1968	41	17

8a. CONTRACT OR GRANT NO.
AF 19(628)-3313

b. PROJECT, Task, Work Unit Nos.
6020-02-01

c. DoD Element 62405394

d. Dod Subelement 681000

9a. ORIGINATOR'S REPORT NUMBER(S)
06093-1-F

9b. OTHER REPORT NO(S) (Any other numbers that may be assigned this report)
AFCRL-68-0383

10. DISTRIBUTION STATEMENT

Distribution of this document is unlimited. It may be released to the Clearinghouse, Department of Commerce, for sale to the general public.

11. SUPPLEMENTARY NOTES

TECH, OTHER

12. SPONSORING MILITARY ACTIVITY
Air Force Cambridge Research Laboratories (CRE), L. G. Hanscom Field
Bedford, Massachusetts 01730

13. ABSTRACT

A research project was planned as a feasibility study to determine whether the X-15 rocket plane could be adapted to carry an instrumented package for pitot measurements. To achieve the desired measurements, a wing pod modification provided the necessary internal volume and external aerodynamic geometry to permit pitot measurements of atmospheric density throughout the altitude range up to 85 kilometers. Five flights, the first two being test flights, were made. Only the third and last flights may be considered useful in deriving results indicative of possible future application of the X-15 for purposes of obtaining reliable data for the pitot measurement. The significant aspects of the research project are the instrumentation associated with the installation of radioactive ionization gages in the X-15, the design of the nose tip configuration compatible with the X-15 wing pod design, and the replacement of original ionization gages with more advanced models. The basic objective of obtaining accurate atmospheric density profiles to expand our understanding of the structure of the upper atmosphere was never fully attained. The present report presents the limitations preventing a successful conclusion of the research as originally conceived. However, the research effort was valuable in pointing out some of the restrictions associated with a manned rocket vehicle.

DD FORM 1 NOV 68 1473

Unclassified

Security Classification

14. KEY WORDS	LINK A		LINK B		LINK C	
	ROLE	WT	ROLE	WT	ROLE	WT
Environmental conditions of supersonic flight						
Atmospheric density measurements						
Pitot sensing system						
Wing pod modification of X-15 for pitot measurements						
Radioactive ionization gages						